



UNIVERSITY OF MINNESOTA
Driven to Discover®



UNIVERSITÄT FÜR BODENKULTUR WIEN
University of Natural Resources
and Life Sciences, Vienna

Influence of debris-flow material composition on the morphology of depositional fans

Author:

Michael Scheiber, BSc

Final Report

Research stay at the Saint Anthony Falls Laboratory, University of Minnesota
from January 31 – July 22, 2022

Supervisors:

Kimberly Hill, Assoc. Prof. PhD
Department of Civil, Environmental, and Geo- Engineering
College of Science and Engineering - Saint Anthony Falls Laboratory
University of Minnesota, Twin Cities, Minneapolis, MN, USA

Roland Kaitna, Assoc. Prof. Dr.
Institute of Mountain Risk Engineering (IAN)
Department of Civil Engineering and Natural Hazards
University of Natural Resources and Life Sciences, Vienna, Austria

Vienna, September 2022

Contents

Abstract	1
1 Introduction	2
2 Objectives and tasks	4
3 Alluvial fans	4
3.1 Background and literature review	4
3.1.1 Fan classification regarding deposition processes	7
3.1.2 Controls on the morphology of debris flow fans	8
3.1.3 Avulsion of debris flows	10
4 Geotechnical tests of relevant “soils” related to debris flows	12
4.1 Material characterization	12
4.2 Slump Slurry tests	12
4.2.1 Methodology	12
4.2.2 Results	17
4.3 Settling tests	20
4.3.1 Methodology	20
4.3.2 Results	22
5 Debris flow fan experiment	22
5.1 Introduction of ongoing project	22
5.2 Debris flow fan experiments	23
5.2.1 Methodology	23
5.2.2 Results: Qualitative comparison of debris flow fans	27
6 Discussion	30
6.1 General interpretation of data from material tests	30
6.2 Discussion on data of debris flow fan experiments	31
7 Conclusion	33
Acknowledgements	34
References	35

Abstract

Debris-flows typically contain a wide range of particles, water, and mud and are hazardous sediment-gravity processes, as they show great variability in size, slope, and surface morphology. There is a great influence of debris-flow composition on the topography of alluvial fans, which understanding in more detail, could support developing new mitigation measures and tools for engineering hazard assessment on mountain regions such for a sustainable land development. The aim of this work was to investigate how changing fine particle content and composition (complementing silt) in debris flows influence flow and deposition dynamics (in particular avulsion) of debris flows, and how these differences in debris flow behavior affect deposition characteristics and the morphology of alluvial fans. To answer these questions, bench-top tests were performed to characterize physical properties of potential debris flow material mixtures where fine particle composition was varied systematically. Using these mixtures, scaled debris flow fan experiments were carried out, where a photogrammetric set-up was applied to capture flow behavior and fan development. Results of material tests suggest that retention of water and retained excess of pore pressure cause viscous effects in slurries when mixtures contain clay and flocculant, but not silt. Silt might not interfere as part of the fluid with sand particles because of its fast settling behavior and therefore could be responsible for higher bulk flow resistance of debris flows. Fan experiments revealed the influence of silt and clay on debris flow behavior as runout and plug formation at the apex affected avulsion patterns as well as deposition characteristics and fan morphology.

1 Introduction

Alluvial fans can be found at the mouths of small and narrow valleys. Different flow processes, including fluvial bedload transport and debris flows transport sediment from the drainage basin downwards to the catchment outlet until it deposits on less steep and wider landscape forming alluvial fans. Their cone-like shaped area, often kilometer across (Hill, 2021) represent suitable sites for settlements and related activities in mountainous areas. Those settlements are mostly protected from flooding of the valley river, but are prone to hazards from the creek related to the fan. Although mitigation cannot guarantee protection in all cases since civil engineering measures are limited and natural hazards vary in recurrence interval and dimension. Those hazards may become more as ongoing climate change effects increasing numbers of extreme precipitation events and permafrost degradation and therefore the number and volume of debris flows increase (e.g. De Haas et al., 2015). This means that alluvial fans represent places of high risk. Hence there is need to further investigate the behavior of flow processes. Better understanding and assessment of those destructive geomorphic processes can contribute to land use planning and natural hazard evaluation and mitigation.

Debris flows deposit on hillslopes, catchments, alluvial fans and channels that can vary greatly in many properties (De Haas et al., 2015). Scientists report that debris flows are the most important sediment-gravity process type with respect to the volume of material delivered to alluvial fans (e.g. Blair & McPherson, 2009; Beaty, 1963) and hence they are a major flow hazard. Yet, different factors responsible for flow behavior and depositional processes of debris flows are discussed in literature. Whipple and Dunne (1992) point out that the morphology of debris-flow fan surfaces is a function of fluvial system efficiency and the temporal frequency of debris-flow occurrence and respective rheologies, volumes, and hydrographs. Those factors also regulate temporal frequency and spatial pattern of channel blockages or episodic shifts. Such episodic shifts of the active channel, also termed avulsion, result in typical semi-conical shape of debris flow fans (e.g Blair & McPherson, 2009; De Haas et al., 2016; Hooke, 1967).

While investigations of some debris-flow properties have already contributed to better flow process understanding, Tsunetaka et al. (2022) recently emphasized further needs to investigate other physical properties of debris flows such as grain size distribution (GSD). Similarly, other scientists (e.g., De Haas et al., 2016; Pederson et al., 2015) point out that the mechanisms regulating shifts or avulsions of debris flows are poorly understood so far.

For that reason, Tsunetaka et al. (2022) recently studied the effect of debris flow GSD on debris-flow forming processes and showed that changing GSD strongly impacts debris-flow fan development and produces varying stratigraphic layers. While effects of GSD of coarse particles in debris flows on flow behavior and deposition geometry is already discussed to some degree (eg. Tsunetaka et al., 2022; Chau et al., 2000, Kaitna et al., 2016), there is only little research available on how the content of fine particles in debris flows controls debris-flow dynamics and the geometry of alluvial fans.

Reports from Whipple and Dunne (1992) indicate that the fine particle fraction (silt-clay) is critical to retention of water within the slurry and, hence, is the most important textural control on flow mobility. Also other research focused on the influence of fine particle fraction on debris flow behavior and fan formation. Kaitna et al. (2016) points out that flow behavior is expected to vary dramatically as GSD varies from mudflows (flows with a high fraction of fine particles) to granular debris flows (flows with a high fraction or large particles). He showed that debris flow mixtures containing a GSD of coarse fraction including fine particles in the fluid strongly influence the presence of sustained excess fluid pressure, which in turn affects bulk flow resistance of debris

flows. Moreover, De Haas et al. (2015) shows that an increase in clay fraction makes debris flow behavior viscous and Chen et. al (2022) demonstrates that increasing fine particle content (clay) correlates with diversity of fan slopes and associated channelization dynamics and also leads to smoother fan surface. Also, Chau et al. (2000) obtained that a mixture containing fines was showing the shortest runout and the least spreading of deposition compared to mixtures with coarser but no fine particles.

Avulsion, which are episodic shifts in the position of a debris-flow channel, are critical for debris-flow fan evolution and for understanding flow hazards because avulsions distribute debris-flow deposits through space and time (De Haas et al., 2018). So far, the mechanisms regulating debris flows shifts or avulsions are poorly understood (e.g., De Haas et al., 2016; Pederson et al., 2015), and a recent publication (De Haas et al., 2018) might be the first systematic study of avulsion mechanisms on natural debris-flow fans. They report two main mechanisms responsible for debris flow avulsion that operate on distinct time scales: (1) *abrupt change* at the time scale of individual surges or flow events and (2) a *gradual shift* of channel and locus of deposition over a longer period of time. Also, several other scientists mentioned factors influencing avulsion processes of debris flows in their studies: Besides the fluvial system efficiency (Denny, 1967; Whipple & Dunne, 1992), also physical properties of debris flows have an influencing character such as temporal frequency (e.g. Whipple & Dunne, 1992; De Haas et al., 2018), rheology (water content, sediment concentration (C_s) and GSD of the source regolith) (e.g. Whipple & Dunne, 1992; De Haas et al., 2018), volumes (e.g. Whipple & Dunne, 1992; De Haas et al., 2018) and peak discharges (hydrographs) (Whipple & Dunne, 1992).

In summary, research indicates the profound effects of GSD, and particularly of fine particle content, in flow material composition on avulsion and depositional behavior of debris flows. Since investigations of De Haas et al. (2015) and Chen et. al (2022) have been focusing exclusively on clay and just a few studies (e.g. Chau et al., 2000; Kaitna et al., 2016) included silt in their fines composition, it might be of further interest to study the role of silt in respect to debris flow behavior and deposition characteristics. One reason for that question is that a debris flow composition in a natural setting mostly also contains silt.

Moreover, although De Haas et al. (2018) were able to improve process understanding of avulsion, there is clearly a need to further investigate avulsion mechanisms and influencing factors. De Haas et al. (2018) also say that poor understanding of avulsion processes might be in part because of a lack of field and experimental data on avulsions.

Therefore, this research aims to investigate the influence of debris flow GSD on avulsion dynamics and depositional characteristics of debris flows. Specifically, investigations on how silt complementing to the fines content affects flow behavior and fan geometry should contribute to better process understanding, which could also help to improve prediction methods and models as mentioned by De Haas et al. (2015).

This research was worked out in the time period from February until September 2022.

2 Objectives and tasks

The overall goal of this study is to better understand the influence of debris flow grain size distribution (GSD) on flow characteristics and the morphology of depositional fans. Specifically, it is of interest to understand how composition and content of fine particle sizes influence flow behavior and deposition characteristics of debris flows and how these are reflected in the topographic signature of alluvial fans. Therefore, the research questions can be summarized as follows:

- (1) How does changing fines particle content and composition (complementing silt) influence flow and deposition dynamics (in particular avulsion) of debris flows?
- (2) How do these differences in debris flow behavior affect deposition characteristics and the morphology of alluvial fans?

To answer these questions laboratory experiments were carried out at facilities of the University of Minnesota. In particular, material tests were carried out in the Multi-phase Fluids and Solids Lab at the Civil Engineering Building to investigate detailed properties and characteristics of potential mixtures used for the scaled debris flow fan experiments. Scaled laboratory debris flow fan experiments were conducted to obtain data of debris flow dynamics and fan building processes at St. Anthony Falls Laboratory (SAFL). Field work on several alluvial fans in Owen's Valley in the White Mountains benefits this work as it served for getting impressions of alluvial fans and depositional processes in a natural setting which helped to better understand and answer research questions.

3 Alluvial fans

3.1 Background and literature review

Generally, alluvial fans are depositional features found at the mouths of side-ravines when sediments transported from catchments are deposited in the less steep and wider, more open landscape of the main valley. They are among the most conspicuous forms of superficial deposits and look like a flat cone, having its apex at the mouth of the ravine (Drew, 1873). Fans deposited by debris flows are often preferred sites for settlements in mountainous areas (e.g. Cavalli & Marchi, 2008) and growing population in mountainous regions has greatly increased the hazardous effects of debris flows (Pederson et al., 2015). De Haas et al. (2018) explains that debris flows that leave the main channel typically pose the largest threat to settlements and infrastructure on alluvial fans, as mitigation measures such as check dams and retention basins are often applied only to the presently-active channels. Investigations of fans can be related to several disciplines and interests such as environmental and geological hazards mitigation, civil engineering, geomorphology, sedimentology, hydrogeology, understanding climate change and more (Blair & McPherson, 2009).

In hydrogeologic respects, alluvial fans are linked to and depend on their drainage basin (also catchment area) and show some general features. Drainage basins basically consist of streams and tributaries which merge to one stream at the lower end of the basin to drain respective area. This merged stream represents a general feature in the basin and is called feeder channel as it feeds the fan with sediment from the drainage basin. Features of alluvial fans are the apex, incised channel, intersection point, active depositional lobe, older surfaces, and headward-eroding gullies (Blair & McPherson, 2009). The apex of a fan is the point at the mountain front where the feeder channel emerges from the catchment (Drew, 1873). The incised channel means the downslope extension of

the feeder channel onto the fan. The intersection point is where an incised channel ends down-fan (Hooke, 1967) and the segment downslope from this point is the region of sediment aggradation which is the site of active depositional lobe (Blair & McPherson, 2009). Blair and McPherson (2009) explain that headward-eroding gullies are common features on the distal fan, particularly in inactive areas away from the active lobe. An overview of general features of drainage basins and alluvial fan is given in Figure 1.

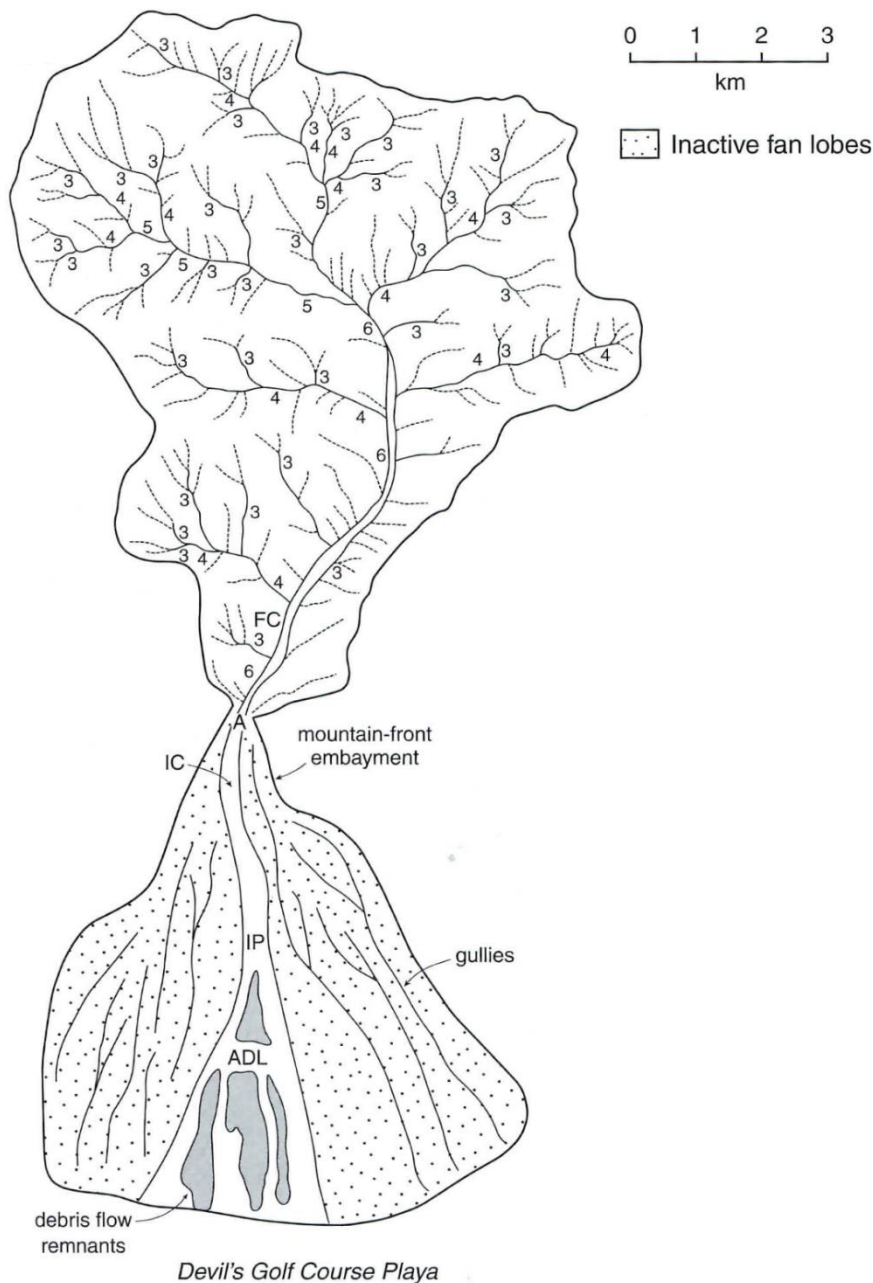


Figure 1: General features of a drainage basin and alluvial fan. First-order channels are not depicted in the catchments due to scale, second-order channels are dashed, and higher-order channels are solid lines labelled by order. The feeder channel (FC) of the catchment leads to the fan apex (A) and other labelled features are the fan incised channel (IC), intersection point (IP), and the active depositional lobe (ADL). Figure after Blair and McPherson (2009).

Apparently, multiple conditions regulate alluvial **fan development**. Blair and McPherson (2009) introduces three conditions necessary for optimal alluvial fan development are: (a) a topographic setting where an upland catchment drains to a valley, (b) sufficient sediment production in the catchment to construct the fan, and (c) a triggering mechanism, usually sporadic high water discharge and less commonly earthquakes, to incite the transfer of catchment sediment to the fan.

When conditions allow fan development, different processes can be responsible for the aggradation of deposition of alluvial fans. Blair and McPherson (2009) introduce primary and secondary processes that transport sediment to and within drainage basins and fans controlling fan development.

Primary processes transport sediment from the catchment to the fan and include rockfalls, rock slides, rock avalanches, earth flows, colluvial slips, debris flows, incised-channel floods, and sheetfloods. They mainly are triggered by intense precipitation or earthquakes, and thus are mostly infrequent and of short duration, but have high impact on fan aggradation (Blair & McPherson, 2009).

Alluvial fans can be built by different primary sediment transport processes. Costa, (1984) and Hungr et al. (2001) list a) fluvial flows and b) different types of debris flows and Blair and McPherson (2009) also mention c) rock-gravity processes as a main fan building process. Primary sediment transport processes can be summarized as:

- a) **fluid-gravity processes** (fluvial flows), generated by failure of colluvial slopes in the catchment, move particles by the force of water
- b) **sediment-gravity processes** (debris flows), generated by failure of colluvial slopes in the catchment, move particles together with fluid by the force of gravity acting directly on the sediment
- c) **rock gravity processes**, generated by failure of bedrock slopes in the catchment, move bedrock by the force of gravity acting directly on the bedrock

Secondary processes on alluvial fans are processes which modify surficial fan sediment in periods between primary processes, including surface or groundwater, wind, bioturbation, neotectonics, particle weathering, and pedogenesis (Blair & McPherson, 2009). Scientists (Whipple & Dunne, 1992; Blair & McPherson, 2009 and Beaty, 1963) emphasize that those secondary processes only have limited importance to fan construction as it affects surface smoothing on a centimeter-to-decimeter scale, but they temporally dominate the fan surface modification due to the infrequency of depositional primary events.

Since this study aims to investigate the morphology of debris flow fans, debris flows as part of the sediment-gravity processes will be introduced. Blair and McPherson (2009) report and Beaty (1963) confirms that debris flows are the most important sediment-gravity process types with respect to the volume of material delivered to alluvial fans. Typical for sediment-gravity processes, debris flows are mostly triggered by water input which generates failure of colluvial slopes in the drainage basin. Water input can happen in the form of heavy precipitation (e.g. thunderstorm), heavy rainfall on water pre-saturated colluvium, or rapid snow or ice melt due to warming (Costa, 1984). Blair and McPherson (2009) describe that debris flow is promoted where colluvium contains mud, because mud induces failure and debris-flow initiation by lowering the permeability of the colluvium, allowing hydrostatic pore pressure to increase and overcome shear strength, leading to the rapid downslope movement of a mud-bearing mass.

Described sediment transport processes can be influenced by several factors. Blair and McPherson (2009) say that fan processes are controlled by at least five factors including catchment bedrock lithology, catchment shape, neighboring environments, climate, and tectonism.

3.1.1 Fan classification regarding deposition processes

For land use planning and hazard assessment purposes around alluvial fan areas, determining the depositional processes responsible for the fans is of great interest. In practice, that is accomplished not just straightforward. Scientists (Marchi & Tecca, 1995; Jackson et al., 1987; Marchi et al., 1993) used different methods to **classify fans** according to their origin depositional processes as fans reveal certain properties and signatures of processes (see below). Alluvial fans are divided into the following three groups: debris-flow fans, entirely fluvial fans, mixed fans. Below, two approaches for fan classification are introduced:

Morphometric approach (Melton, 1965)

- Fan area: planimetric area of the fan
- Fan slope: average slope of the fan surface along its bisector (apex to toe)
- Ruggedness number (Melton number) as the ratio of
 - Drainage basin height: elevation difference between the highest and the lowest point (=fan apex) in the drainage basin, and the square root of
 - Drainage basin area: planimetric area of the drainage basin
 -
- Chart comparison of fan slope with drainage basin and height (Melton number) (Jackson et al., 1987)

Following criteria values indicate **debris-flow fans**. If values don't meet or lack criteria, fans tend to be of fluvial **origin**.

- Melton number $>0.25-0.30$ (Marchi & Tecca, 1995)
- Drainage basin areas $< 20-30\text{km}^2$ (Marchi et al., 1993)
- Fan slope $>4^\circ$ (Jackson et al., 1987)

Field observation approach

Costa (1988) suggests using following geomorphic and sedimentologic criteria and parameter to classify fans:

Geomorphic and sedimentologic criteria for **debris-flow genesis**:

- Exposures of debris flows diamictions
 - Weak stratification
 - Poor sorting
 - Matrix supported angular clasts
- Exposures on the fan surface – indication debris-flow genesis
 - Levees
 - Lobes
 - Boulders ($>1\text{m}$ diameter)

Geomorphic and sedimentologic criteria of **fluvial deposits**:

- Exposures of fluvial flow deposits
 - Stratification visible
 - Moderately to well sorted
 - rounded clasts

Complementing data for fan classification

- Historical data (Marchi et al., 1993)
- local morphological evidence (Marchi et al., 1993)

Following *Table 1* summarizes methods and their criteria and parameters for fan classification.

Table 1: Methods and criteria for fan classification

method	Criteria and parameter	Origin processes of deposits	
		Debris flow	Fluvial
Morphometric	Melton number	>0.25-0.30	<0.25-0.30
	Drainage basin area	<20-30km ²	>20-30km ²
	Fan slope	>4°	<4°
Field observations	Stratification	Weak/unstratified	stratified
	Sorting	Poor sorted	Moderately to well sorted
	Clast fabric	Matrix supported angular clasts	Rounded clasts
	Levees on fan surface	Present	Not present
	Lobes on fan surface	Present	Not present
	Boulders >1m on fan surface	Present	Not present

3.1.2 Controls on the morphology of debris flow fans

Since deposition processes affect fan building, it also regulates the **fan surface morphology**. The depositional morphology of debris-flow fan surfaces is most directly affected by the “strength” of the **fluvial system** and the **physical properties of debris flows** such as temporal frequency of debris-flow, volumes, and peak discharge (Whipple & Dunne, 1992).

Whipple and Dunne (1992) explain that, where fluvial sedimentation might contribute little to the aggradation of alluvial fans, **fluvial processes** can play a critical role in the construction of the fans by eroding channels through the debris-flow deposits. They therefore explain that **channels** on a debris-flow fan can be built by self-confinement of debris flows between their own levees but also by channel scour by floodwaters or debris flows. In other words, these channels can be produced by erosional processes or levée aggradation.

Fluvial processes control channel size and down-fan extent, the likelihood that a recently deposited channel plug will be scoured away, and the duration of the interval between channel blockage and the establishment of a new, continuous channel course (Whipple & Dunne, 1992). Thus, they say, that networks of channels arise from repeated avulsions of a single channel, driven by deposition of high sediment concentration (C_s) debris flows.

Moreover, Whipple and Dunne (1992) describe that the morphology of the fan surface, partly controlled by spatial pattern of debris-flow deposition, is further influenced by **channels conveyance capacity** but also **physical properties** of the debris flow. For instance, some debris flows traverse the entire length of the fan whereas others come to rest after a short transport

distance somewhere on the fan. Physical properties are relevant because debris flow confinement (within channels) and conveyance farther down-fan depends on relative peak discharge (hydrographs) magnitudes and the conveyance capacity of the channel, which in turn corresponds to flow rheology as well as channel size and gradient (Whipple & Dunne, 1992).

Abovementioned **physical properties** of debris flows have great morphological consequences for debris flow deposition. Physical properties of debris flows are controlled by temporal frequency, rheology (water content, sediment concentration and GSD of the source regolith), volume and peak discharge (e.g. Whipple & Dunne, 1992). Those properties have been discussed by several scientists.

As for **sediment concentration** C_s , which is the ratio between sediment weight (all particles) and fluid weight (water), it directly relates to water content. For instance, a typical field-scale water content would vary between 15 and 30% by weight (Iverson et. al, 2011). Whipple and Dunne (1992) report that debris-flow behavior changes with C_s and results in diverse spatial deposition signatures such as runout distance, flow velocity, lateral shifting, boulder transport capacity, change of channel system, etc. For instance, debris flows with high- C_s are only mobile on relatively steep slopes ($>4.5^\circ$) and are therefore limited mainly to the steeper reaches up-fan where they deposit as a relatively thick mass flow (Whipple & Dunne, 1992). In contrast, debris flows with relatively low- C_s have limited boulder-transport capabilities and traverse gentle slopes (1° - 2°) (Whipple & Dunne, 1992). Also, Chau et al. (2000) reports from debris flow experiments, where findings show, that flows with higher water content (meaning lower C_s) always result in a more mobile debris flow and longer runout. Those flows are dictated largely by the condition of the channel system it encounters as they can rapidly move down-fan or be trapped behind a channel plug and might spread laterally when escaping a channel, leaving behind thin sheets of deposits in both cases (Whipple & Dunne, 1992).

As further mentioned by Whipple and Dunne (1992), another property controlling debris flow behavior is **GSD**, which can vary among the different drainage basin lithologies. Literature therefore lists a range for GSD for debris flows. As one example, Hubert and Filipov (1989) investigated debris flows deposits in alluvial fans on the west flank of the White Mountains averaging 60% gravel, 25% sand, 11% silt and 4% clay.

The important role of GSD in debris flow processes is also supported by Tsunetaka et al. (2022), who found in debris flow experiments (GSD including no fine particle), that varying GSD is closely related to spatial diversity in fan morphology stratigraphy. Contributing to this, Chau et al. (2000) found that a change in granular content (from high fines to higher coarse particle content) but fixed water content, increased runout distance by 350% and also the shape and area of fan altered correspondingly in their experimental debris flows. Interestingly, the finest mixture, containing gravel, sand but also silt & sand, was showing the shortest runout and the least spreading of deposition compared to the mixtures with coarser particle content (sand and gravel).

However, Whipple and Dunne (1992) argue that the **fine particle fraction** (silt-clay) is critical to retention of water within the slurry and, hence, is the most important textural control on flow mobility. Scientists investigated the influence of GSD on flow behavior considering not only coarse but also fine particle fraction. Debris flow experiments by De Haas et al. (2015) revealed that runout enhanced with an increase in clay fraction, probably because of better retained excess pore pressures. But his examinations also showed that too large proportions of clay (>0.22) make debris flows highly viscous so that runout is reduced. Kaitna et al. (2016) report that debris flow behavior, in part described by flow resistance, is expected to vary dramatically as the grain size distribution contains higher fractions of fine (clay and silt) or coarse particles (gravel and boulders). Most recently, Chen et. al (2022) demonstrated the importance of fine particle content as the increase of

clay content decreases diversity of fan slopes and associated channelization dynamics and therefore leads to smoother fan surface.

3.1.3 Avulsion of debris flows

Repeated sediment deposition by debris flows is responsible for the formation of debris-flow fans. The semi-conical shape of those debris flow fans is obtained by episodic shifts of the active channel from a fixed fan apex (e.g., Blair & McPherson, 2009; De Haas et al., 2016; Hooke, 1967). Those episodic shifts in the position of a debris-flow channel, termed **avulsions**, are critical for debris-flow fan evolution and for understanding flow hazards because avulsions distribute debris-flow deposits through space and time (De Haas et al., 2018). So far, the mechanisms regulating debris-flow shifts or avulsions are poorly understood (e.g., De Haas et al., 2016; Pederson et al., 2015). De Haas et al. (2018) say this might be in part because of a lack of field and experimental data on avulsions.

Several scientists mentioned avulsion processes of debris flows in their studies and tried to describe the potential mechanisms behind. E.g., De Haas et al. (2018), observed two main mechanisms responsible for debris flow avulsion that operate on distinct time scales: (1) **abrupt change** at the time scale of individual surges or flow events and (2) a **gradual shift** of channel and locus of deposition over a longer period of time.

Regarding **mechanism (1)**, Beaty (1963), obtained and described the phenomena of channel changes as a result of plugging of active channels by large boulders. He argues that the channel change process is particularly evident where a number of channel-plugging boulders were found, behind which rubble had piled up until channel walls were overtopped and the floods and debris flows swerved to one side or the other and continued down the fan along new courses.

Also the finding from Hubert and Filipov (1989) support this avulsion mechanism as they described that debris-flow surges, developed from breaching of temporary dams made of debris in the channels, can in some cases lead to flow shifting course out of the channel.

In agreement with findings from Hubert and Filipov (1989), a recent study from De Haas et al. (2018) described mechanism (1) as an abrupt change in channel position at the time scale of individual surges or flows, likely driven by the occurrence of channel plugs which force subsequent flows to avulse.

As for **mechanism (2)**, Whipple and Dunne (1992) report that channels are often blocked by deposition of debris flows, which plays an important role in the long-term evolution of the channel system and in the dispersal of debris-flow sediments across the fan. It affects fan surface morphology as it impacts fan channelization such as channel blockage, up-fan aggradation and channel in-filling, followed by channel diversion Whipple and Dunne (1992). They explained that channel blockage is regulated by the fluvial system efficiency and the temporal frequency of debris-flow rheologies, volumes, and hydrographs. They infer that new channels are cut in response to channel blockage by high-Cs debris flows and floodwaters are diverted around recently deposited debris-flow plugs, resulting in avulsion of the channels. Final flow diversion to a new channel is not accomplished instantaneously as localized deposition builds up over some time behind the blockage and up-fan so that new channel courses, therefore, rarely diverge immediately behind the channel plugs, but rather some distance up-fan (Whipple & Dunne, 1992). De Haas et al. (2018) called it a gradual shift in the predominant transport pathway and locus of deposition over the time scales of multiple flows. Hereby, the average locus of debris-flow deposition gradually shifts toward the topographically lower parts of a fan highlighting the importance of topographic compensation for long-term avulsion behavior and flow-path selection. Their findings indicated that channel plugs can form in flows of all volumes, whereby flows with

low mobility, either caused by small volume or flow composition, are especially likely to plug a channel and induce avulsion. They also say-, that-, channel plug formation and their occurrence likely depends at least in part upon flow composition and bulk rheology as well as flow volume. Furthermore, they explained that plugs were observed to mostly form in small to moderate flows, especially those that deposit material. After plugs are formed, following small to moderate size flows will deposit material behind the plug, filling the channel and leading to progressive backstepping of the locus of debris-flow deposition (De Haas et al., 2018). This continues until a debris flow occurs of sufficient volume to leave the main channel and establish a new channel, they argue. This underpins that the magnitude-frequency distribution of debris flows feeding a fan, as well as the order in which small, moderate, and large flows occur, may exert a strong control on the spatio-temporal evolution of debris-flow fans (De Haas et al., 2018).

Thus, those findings suggest-, that avulsion due to channel plugging generally follow a coherent pattern of, backstepping, avulsion and establishment of a new active channel, perhaps accompanied by incision into older deposits (De Haas et al., 2018).

Contributing to findings from De Haas et al. (2018), quasi-cyclic alternations of avulsion, channelization and backstepping of the active depocenter have also been documented on small-scale experimental debris-flow fans by De Haas et al. (2016).

Also another study indicated that spatio-temporal shifts of the locus of deposition on natural debris-flow fans may show patterns of backstepping and avulsion (e.g., Dühnforth et al., 2007).

A contribution in different regards to avulsion mechanisms mentioned the role of headward erosion of gullies. Denny (1967) points out, that headward erosion of gullies either as single channels or a downslope-converging network, may eventually progress sufficiently upslope to intersect the incised channel, possibly causing autocyclic switching of the active depositional lobe to another part of the fan.

Most recently, a study from Tsunetaka et al. (2022) reports that differences in debris flow GSD may cause more avulsion for multi-granular flows than for mono-granular ones which in turn result in different fan forms. This might agree with Whipple and Dunne (1992) and De Haas et al. (2018) who mention, that debris flow debris-flow properties (flow composition and bulk rheology) are influencing avulsion of debris flows.

In summary, abovementioned findings revealed some potential factors which might at least in part influence the mentioned avulsion mechanisms. Besides the fluvial system efficiency (Denny, 1967; Whipple & Dunne, 1992), following physical properties of debris flows have an influencing character:

- temporal frequency (e.g. Whipple & Dunne, 1992; De Haas et al., 2018)
- rheology (water content, sediment concentration (C_s) and GSD of the source regolith) (e.g. Whipple & Dunne, 1992; De Haas et al., 2018; Tsunetaka et al., 2022)
- volumes (e.g. Whipple & Dunne, 1992; De Haas et al., 2018)
- peak discharges (hydrographs) (Whipple & Dunne, 1992)

4 Geotechnical tests of relevant “soils” related to debris flows

In order to characterize relevant soils and fluids in the context of debris flow material, various tests were carried out in the laboratories of the University of Minnesota. Specifically, Slump Slurry tests and settling tests were carried out.

The methodology and experimental set-up of **Slump Slurry tests** is in parts similar to the so-called Flow Table Test for testing fresh concrete (Austrian Standards, 2019). While a concrete slump test serves to quantify a metric of how a certain concrete mixture spread after the slump, the Slump Slurry tests similarly should help to quantify material mixture characteristics.

Slump Slurry tests were conducted to find out more about material flow behavior of different material composition. In general, mixtures of sand, silt, clay and water were used to simulate debris flow material.

Settling tests were executed for further characterization of tested material compositions. Hereby, the settling of particles over time was documented.

4.1 Material characterization

Material characterization tests of various soil mixtures served to better understand the physics and dynamic processes in material mixtures but also to find potential debris flow compositions for laboratory experiments. Here, Slump Slurry tests and settling tests were carried out.

In this study, sand, silt, clay, Polydiallyldimethylammonium chloride (PDADMAC), which is used as a flocculant to enhance settling of clay particles, and water were used for different mixture compositions. The range of grain sizes for sand (specific gravity 2.65 g/ml) was 4mm-0.063mm. For the smaller particles, special silt (specific gravity 2.60 g/ml), which is non-hazardous for experimental use, and Kaolinite (specific gravity 2.65 g/ml) were used. In general, sand was considered as the solid fraction and water, silt, clay and PDADMAC built the fluid part of the mixture.

4.2 Slump Slurry tests

4.2.1 Methodology

For the Slump Slurry tests, the compositions basically were divided into 8% (group 1) and 16% (group 2) fines/fluid by mass. For each group, 5 mixture compositions have been tested where their fines content was kept the same but the fines composition (clay and silt) changed. Also see *Table 2*.

The composition of the mixtures oriented on the study from Chen et. al (2022) so that in this study the volumetric ratio solid/fluid = 27.40/72.60 for all material tests. This volumetric ratio results from a reference mixture without any fines (series 1), where sand and water were mixed in a ratio solid/fluid = 50/50 by mass.

The proportion of the solid and fluid fraction of the mixture depend on the volume ratio solid/fluid = 27.40/72.60 which gives each series a slightly different ratio by mass (e.g. mixtures 8% fines/fluid: solid/fluid = 48.7/51.3; mixtures 16% fines/fluid: solid/fluid = 47.4/52.6;). Furthermore,

all mixtures were mixed for a total volume of 200 ml so that the slurry, more or less, did not run off the metal board where the tests were performed on.

As mentioned earlier, PDADMAC (flocculant for clay particles) was added for most of the tests. To test the different impacts of flocculant and its amount, flocculant as part of the fluid was varied within each series and made up 1%, 0.5%, 0.1% or 0% of the fines mass. This means that for each series up to four different composition were tested.

In particular, series 2 and 4 contained all four different flocculant mixtures, series 3 and 6 included mixtures with 1%, 0.1% and 0% and neglected the mixture with 0.5%. This was because results from series 2 and 4 showed no real difference between the 1% and 0.5 % mixture. For series 5, 7, 8, 9, 10 and 11 also the mixture without any flocculant was neglected because previous results showed, there was no doubt, that flocculant would not influence slump slurry result. Therefore focus on mixtures with flocculant. Therefore, those series were carried out only for 1% and 0.1% flocculant.

Hence, 10 different series were tested and considering that the series included different amount of flocculant, as explained above, tests of 26 different mixture compositions were carried out.

Moreover, for reasons of tests reliability, each mixture composition was tested three times (test A,B and C) in a consistent manner to minimize random test results. Thus, in total there have been 78 tests carried out.

Table 2: Overview of the mixture compositions

	Mixture name	sand % by mass	fluid % by mass	water % per fluid	clay % per fluid	silt % per fluid
series 1	water	50.00	50.00	100	0	0
Group 1: Compositions with 8% fines/fluid						
series 2	Clay8_0-1F	48.72	51.28	92	8	0
	Clay8_0-5F	48.72	51.28	92	8	0
	Clay8_0F	48.72	51.28	92	8	0
	Clay8_1F	48.72	51.28	92	8	0
series 11	Clay6Silt2_0-1F	48.73	51.27	92	6	2
	Clay6Silt2_1F	48.73	51.27	92	6	2
series 4	Clay4Silt4_0-1F	48.73	51.27	92	4	4
	Clay4Silt4_0-5F	48.73	51.27	92	4	4
	Clay4Silt4_0F	48.73	51.27	92	4	4
	Clay4Silt4_1F	48.73	51.27	92	4	4
series 10	Clay2Silt6_0-1F	48.73	51.27	92	2	6
	Clay2Silt6_1F	48.73	51.27	92	2	6
series 3	Silt8_0-1F	48.74	51.26	92	0	8
	Silt8_0F	48.74	51.26	92	0	8
	Silt8_1F	48.74	51.26	92	0	8
Group 2: Compositions with 16% fines/fluid						
series 5	Clay16_0-1F	47.38	52.62	84	16	0
	Clay16_1F	47.38	52.62	84	16	0
series 9	Clay12Silt4_0-1F	47.39	52.61	84	12	4
	Clay12Silt4_1F	47.39	52.61	84	12	4
series 8	Clay8Silt8_0-1F	47.39	52.61	84	8	8
	Clay8Silt8_1F	47.39	52.61	84	8	8
series 7	Clay4Silt12_0-1F	47.40	52.60	84	4	12
	Clay4Silt12_1F	47.40	52.60	84	4	12
series 6	Silt16_0-1F	47.41	52.59	84	0	16
	Silt16_0F	47.41	52.59	84	0	16
	Silt16_1F	47.41	52.59	84	0	16

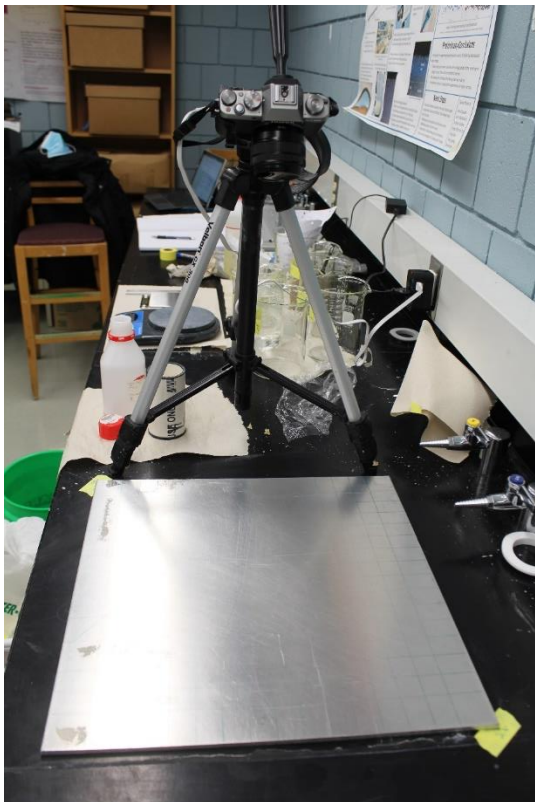


Figure 2: Experimental set-up for the Slump Slurry tests: a) containers and scales used for mixing the mixtures; b) metal board and camera set-up on a tripod; c) bottle and cylinder

Figure 2 shows the experimental set-up of the Slump Slurry tests. Different containers, precisely labeled to prevent any mix ups, were used to weigh and mix the materials. A high precision (0.00g) scale and another scale (0g) made precise mixing possible. Metal rulers and syringes were useful to pour and weigh the flocculant.

The plastic bottle (volume >200ml) was used to shake and well mix the materials. Next to it, the cylinder (volume >200ml) was placed in the center of the metal board and served to pour in the mixture. The cylinder's cross sections are covered with a ring (black) of rubber or membrane like material for leak proof connection to the board during the pouring process.

The metal board was of square shape and its size was ~16 inches (40.65cm). The board was covered by a pattern of squares, each one inch in length, which served for calibration and data processing. A camera fixed on a tripod was used to document the data.

In order to conduct the Slump Slurry tests and for having a good overview, the different mixture compositions were calculated. The calculation of the solid and fluid fractions based on information about composition, volume ratio, volume and material densities for each mixture.

As for the flocculant, which is calculated as percentage of the fines mass and therefore resulted in relatively small amounts, it was necessary to separately calculate a dilution procedure. This means, the amount of flocculant added to the mixture was too little to weigh so that a greater amount of flocculant, sufficient to weigh with a scale, was diluted with a great amount of water as well to have the correct concentration of flocculant in the water. For the test itself, just a little amount of that relatively big volume was used finally.

The experimental procedure started with adding the different amounts of materials into the small bottle. Therefore, sand was added followed by fines (clay and/or silt), water with/without flocculant. Making sure, the metal board and the tube is in position, the bottle got shook for around 1-1.5 minutes. After shaking the bottle properly, it was opened quickly and the mixture was poured into the cylinder. As soon as the tube was filled, it got lifted up so that the mixture slumped out and built a slurry on the metal board. The result was documented with a camera which was fixed on a tripod and notes were taken. Finally, the board, tube, membrane and surfaces were cleaned up and everything was ready for the next experiment. All tests were conducted in a consistent manner.

Some metrics needed to be defined for the slurry to evaluate mixture characteristics. The Slump Slurry data was processed in a quantitative approach where perimeter and area of slurries were obtained for further data analyses.

In order to obtain the area and perimeter, MATLAB was used in a first step for distortion correction of the Slump Slurry photos. Secondly, the perimeter of each slurry was obtained by drawing the perimeter of the original sized and distortion corrected slurry photo on a touchpad manually. Having those clear perimeter drawings on white background made it possible to obtain and calculate A and P in MATLAB.

During data processing it appeared, that for mixture Clay2Silt6_0-1F_C the calculated values A and P were not correct. Also, results from other mixtures (Silt8_1F_B, Silt8_1F_C, Clay4Silt4_0F_C and Clay4Silt12_1F_A) were not considered in the calculation due to the fact, that some part of their slurry were far off the plate so that the camera did not capture the whole slurry. However, that did not affect the data process as the experimental procedure was conducted three times (A, B and C) for each mixture. In other words, reliable results for each mixture could be calculated.

Moreover, since the manual drawing approach includes variation and randomness, a few perimeters were drawn twice so that a comparison of P can give an idea about human error in this process.

In general, it was of interest to analyze the Slump Slurries regarding:

- a) the influence of fines composition (clay, clay + silt, silt)
- b) the influence of fines content per fluid (8% or 16% fines)
- c) the influence of different amounts of flocculant (0.1% and 1%)

Processed data of A and P were analyzed in two ways:

1) Calculated values for A and P were each brought into relationship with the content of clay and silt for mixtures 8% and 16% fines/fluid. Potential trends were statistically calculated by linear regression.

2) Calculation of the complexity index N_b for mixtures with 0.1% and 1% Flocculant, which quantitatively assesses local surface irregularities (e.g. shape of perimeter). The complexity index was used in a latest study from Chen et. al (2022) as $N_b = P^2/(2A\Delta\theta)$, which was drawn from Hill et. al (1999) and Hill et. al (2004). N_b is dimensionless and describes a relationship between a circle-like and irregular perimeter, where A stands for the total spreading area, P for the length of perimeter and $\Delta\theta$ is the angle of a slurry segment. Here, $\Delta\theta$ was 2π since the slurries represented full circles for the calculation.

N_b was plotted in triangle plots (Python) to obtain variations and potential relationships among the mixtures. The triangles' corners are regarding the mixture compositions where the corners from left-top-right represent following parameters: 100% silt/fluid - 100% clay/fluid - 100% water/fluid

4.2.2 Results

Figure 4 showed that the range of N_b values for mixtures of 1% flocculant/fines (range = 4.59) was wider than for 0.1% flocculant/fines mixtures (range = 2.47). Furthermore, values for group 2 were smaller than for group 1 for mixtures of 0.1% as well as 1% flocculant/fines. Moreover, there are trends for N_b to increase with the proportion of silt/fluid and decrease with the amount of clay/fluid respectively. Along with that, N_b for clayey mixtures ($\geq 50\%$ clay/fines) basically do not vary much (range = 0.44) and show noticeably lower values than silty mixtures. This is true for mixtures of 0.1% and 1% flocculant/fines, whereas there was even a greater difference (jump) in N_b values between clayey and silty mixtures when mixtures contained 1% flocculant/fines. Mixtures consisting of silt only and no clay showed the highest values although N_b for the mixture of 16% silt containing 1% flocculant/fines ($N_b = 3.46$) is only slightly greater than for the mixture

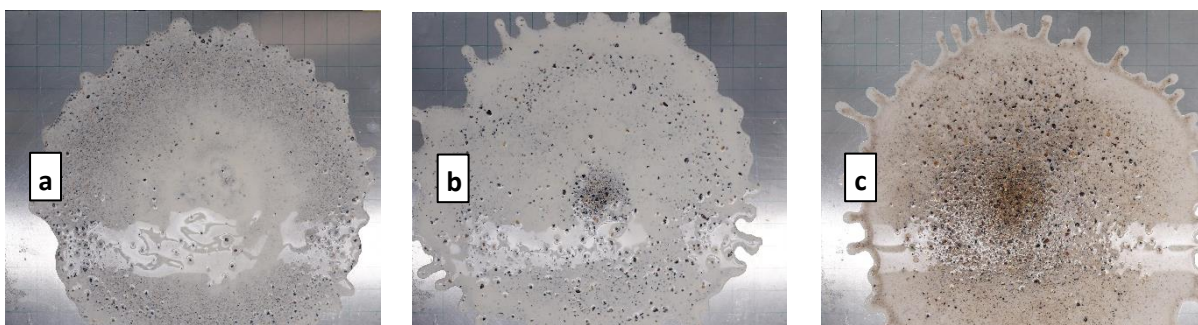


Figure 3: Slurry results for mixtures Clay8_0-1F (a), Clay8_0F (b) and Silt8_0-1F (c)

12% silt and 4% clay containing 1% flocculant/fines ($N_b = 3.34$). Comparison of (a) and (b) regarding their 8% and 16% fines/fluid mixtures show that N_b values more or less were of same magnitude, whereas there were relatively high values (i.e. 4.44 and 6.27) for 1% flocculant mixtures of 8% fines/fluid.

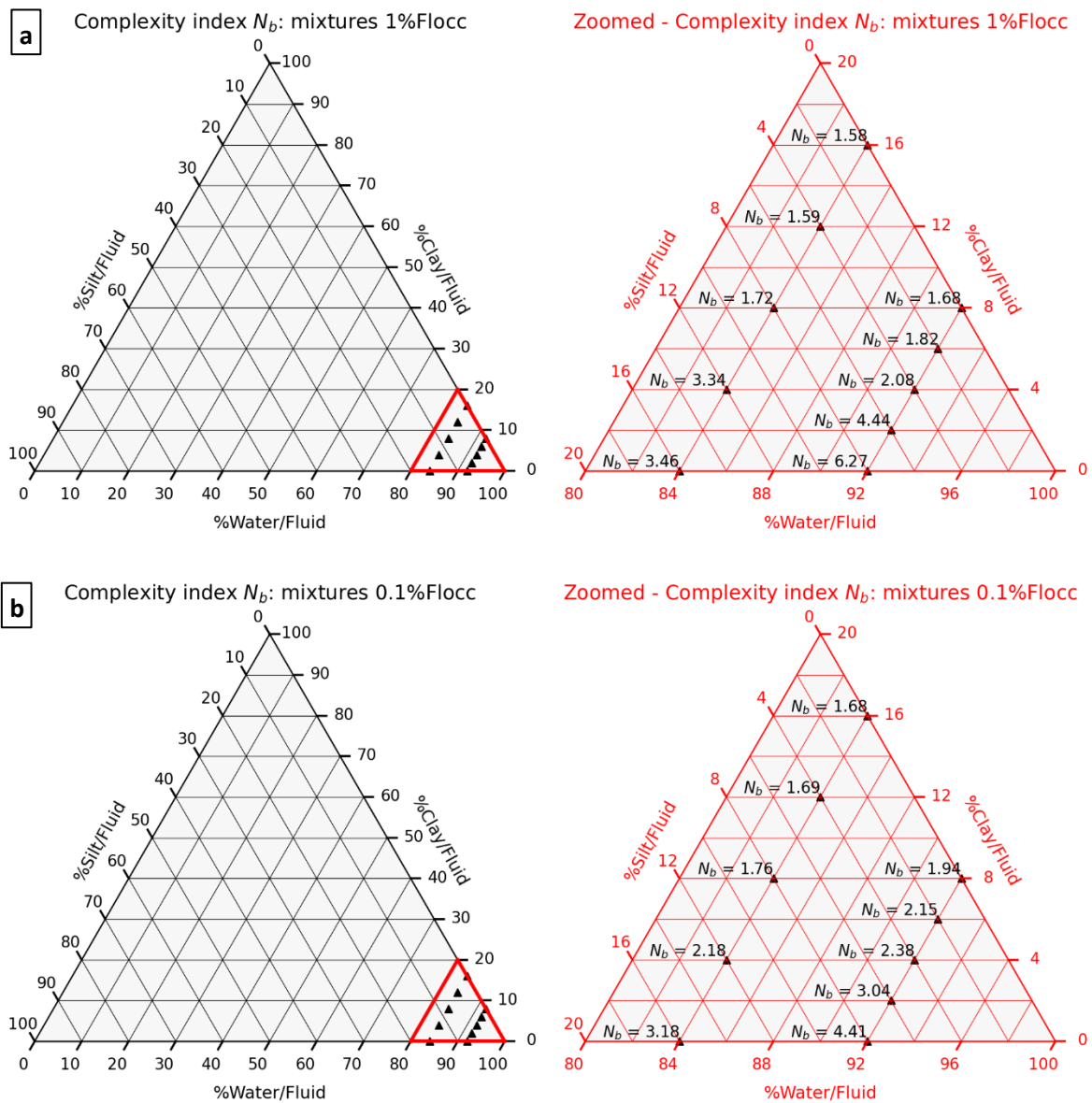


Figure 4: Triangle plots (silt – clay – water) showing the calculated complexity index N_b (small, bold triangle symbols) for mixtures of different flocculant content: (a) mixtures containing 1% flocculant/fines and (b) mixtures containing 0.1% flocculant/fines. Plots on the left serve as overview and red triangles on the right display a zoomed plot to show the location of N_b according to the mixtures' material composition (silt, clay and water). Triangles along the 92% water/fluid line display N_b values for 8% fines/fluid (group 1) and triangles along the grid line of 84% water/fluid show data for 16% fines mixtures (group 2).

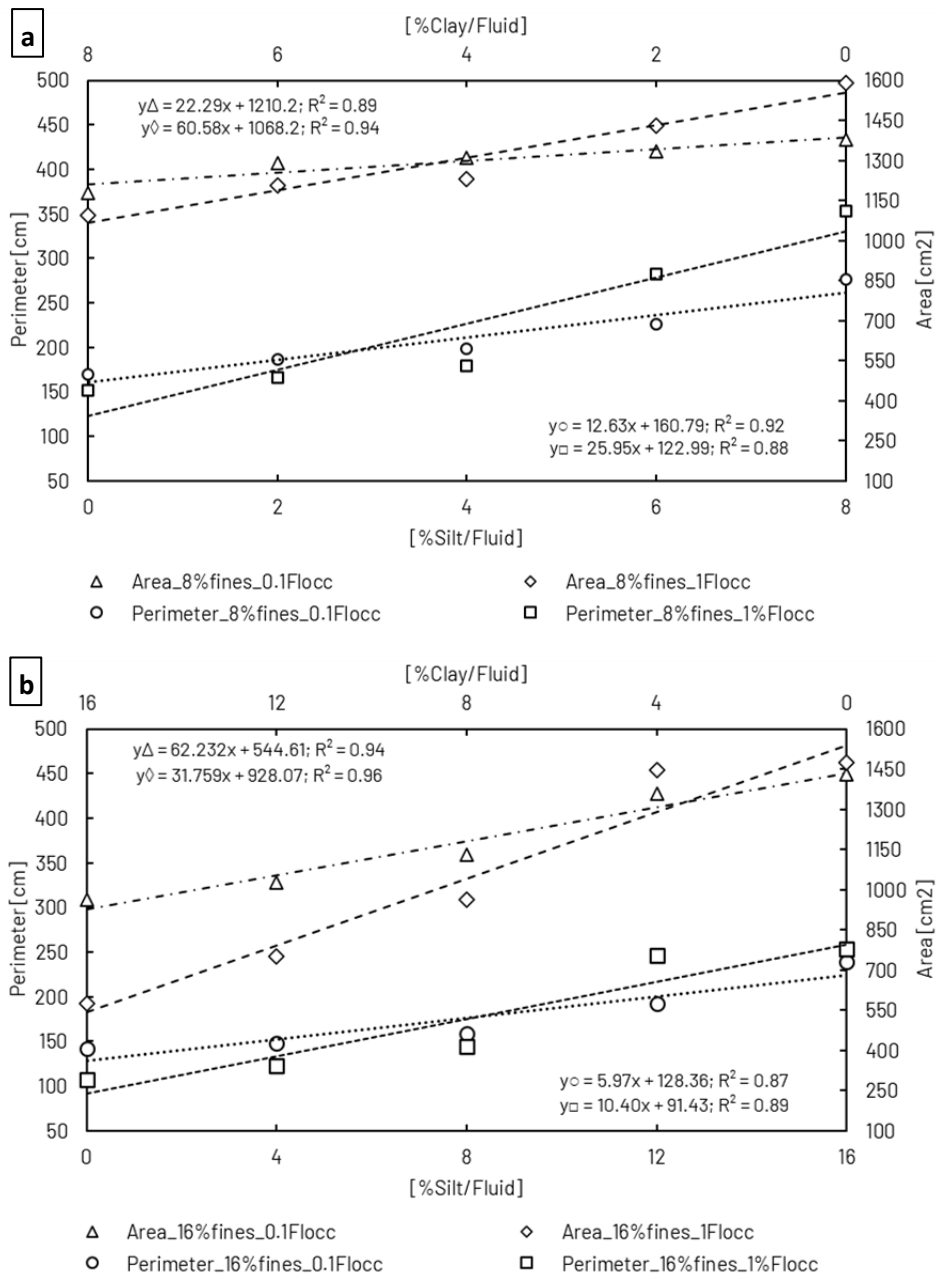


Figure 5: Results of area and perimeter depending on mixture's silt and clay content (bottom and top horizontal axis) for (a) mixtures of 8% fines/fluid and (b) 16% fines/fluid considering results for both 0.1% and 1% fines/fluid mixtures

Overall, both graphs showed trends for area and perimeter to increase with the proportion of silt/fluid and decrease with the amount of clay/fluid respectively. For graph (a) as well as for (b) it is true that area increased with a higher gradient than perimeter did.

Moreover, results of area and perimeter exhibited higher values for mixtures of 8% fines/fluid than for 16% fines/fluid mixtures.

Area of clayey mixtures containing 1% flocculant/fines in (b) were much lower compared to (a). Mixtures of 0.1% flocculant/fines exhibit higher values for area and perimeter compared to mixtures of 1% flocculant/fines when mixtures were clayey ($\geq 50\%$ clay/fines) but lower values when silty ($> 50\%$ silt/fines).

4.3 Settling tests

4.3.1 Methodology

As part of the material characterization tests, four settling tests were performed in total (see *Figure 6*). The compositions of the mixtures followed defined ratios and volumes from the Slump Slurry tests (solid/fluid = 27.40/72.60 by volume; Volume = 200ml). Tests were carried out for mixtures containing 8% fines only, because findings from Slump Slurry experiments indicated that mixtures containing 8% fines would mimic appropriate material behavior for planned debris flow fan experiments. Therefore, following compositions were tested in settling tests:

- Clay8_0%F
- Clay8_0.1F
- Silt8_0.1F
- Clay4Silt4_0.1F

This means, tested mixtures differed as the fines particle composition varied from 8% clay/fluid without flocculant, 8% clay/fluid with 0.1% flocculant/fines, 8% silt/fluid with 0.1% flocculant/fines and 4% clay + 4% silt/fluid with 0.1% flocculant/fines.

The experimental set-up for the settling tests was partially similar to the Slump Slurry as the tools for preparing the mixtures were the same. The settling tests, however, required some sort of small but high containers where the mixture can settle under undisturbed conditions. Here, four identical glass cylinders having a volume of >250ml were used for the settling tests. The cylinder's scale bar [ml] served to quantify the settling rate [volume/time]. The cylinders were positioned on a table with a black background for better transparency for photos and an additional ruler served for metric scale. A camera fixed on a tripod was used to document the data during the settling process.

Calculation and mixing procedure were analogous to Slump Slurry tests (chapter 4.2.1). The camera was in position and a video was started to capture all the settling processes. The procedure generally consists of two steps: 1) in a first step the mixture was mixed and after shaking the bottle, the mixture was poured into the first cylinder (Clay8_0%F). This was repeated for the other three mixtures (Clay8_0-1F, Silt8_0-1F, Clay4Silt4_0-1F) as well; 2) Some piece of rubber was used to cover the cylinder's open end to again shake the whole cylinder with its mixture inside. The cylinder was shook for around 30 seconds and the settling experiment started when the cylinder was placed on the table. Right after that, this procedure got repeated for the other three mixtures. According to step 1) and 2), the four settling experiments were started time delayed. In particular, the time difference between two mixture tests was around 1:10 minutes, so that the time difference between the start of the first (Clay8_0-1F) and the last mixture (Clay4Silt4_0-1F) was around 3:25minutes.

During the settling process, it was of interest to obtain data regarding any particle segregation. Therefore, notes were taken as far as layers were built during the deposition of particles. Those notes considered the vertical position [ml] of those borderlines of layers at the corresponding time. To prevent any transpiration during the duration of the settling tests (24 hours), the cylinders were covered at the open end.

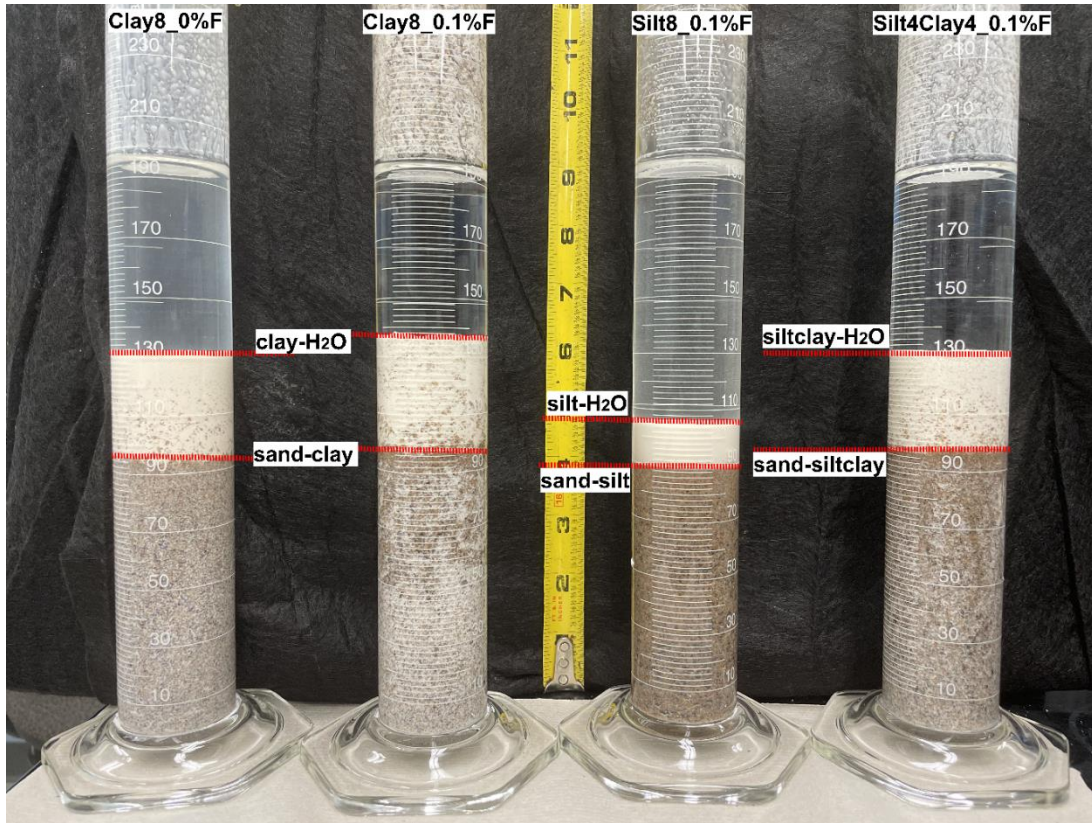


Figure 6: Settling tests for the four mixtures after 24 hours. Dashed lines in red represent borderlines between the particle layers.

For presenting data, settling rate [volume/time] for each mixture and layer are visualized showing trends of settling processes for the different layers of mixtures.

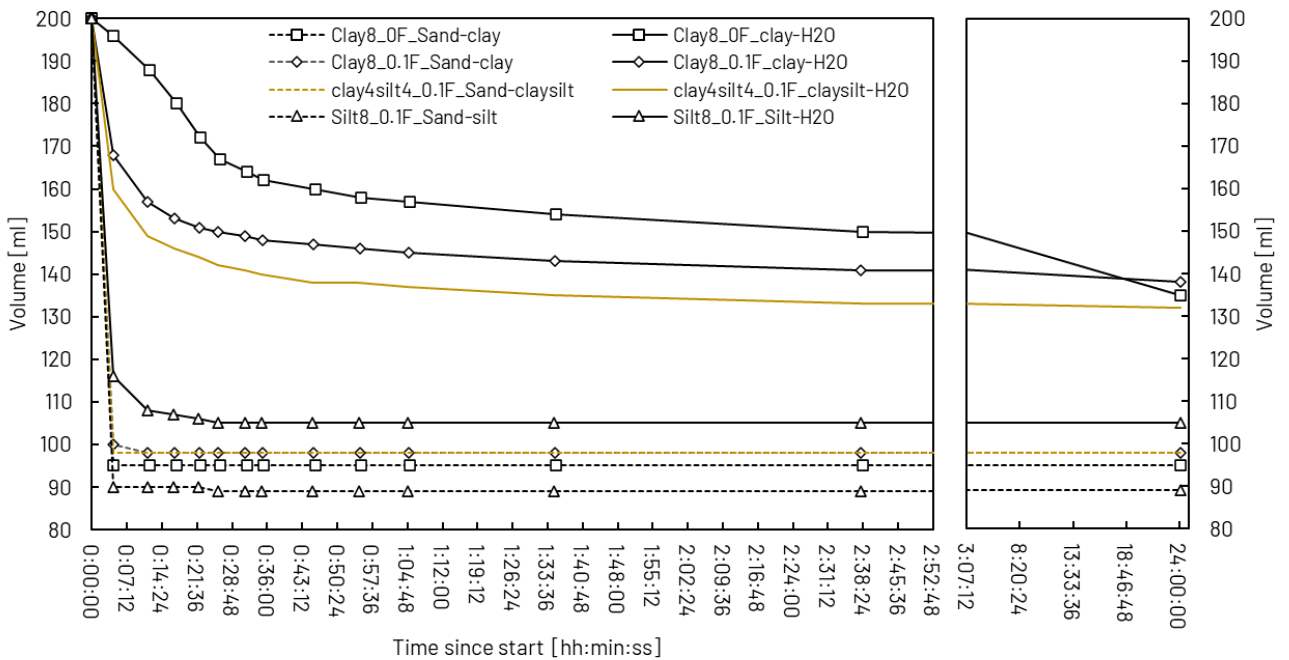


Figure 7: Settling trends showing the vertical position [ml] regarding time [hh:min:ss] for segregation layers of 4 different mixtures. Solid lines represent borderlines between settled fines particles and water (H2O) and dashed lines show borderlines between sand (on the bottom) and fines particles.

4.3.2 Results

Plot of settling trends (*Figure 7*) mainly focuses on the beginning of the experiment (first 2:50 hours) after which most particles finished settling down. Additionally, the final settling states at 24 hours after start were added to the plot.

Results show fast settling of sand (dashed lines) within the first minutes of the experiments for all mixtures, forming a sand layer at the bottom of the cylinder. After that time, basically only the layers consisting of fines particles continued settling.

Regarding those fines particles, settling for silt particles of the mixture Silt8_0-1F occurred fast so that particles were completely settled after around 30 minutes. In contrast, settling of fines particle mixtures consisting clay (Clay8_0%F, Clay8_0-1F and Clay4Silt4_0-1F) continued settling until 24 hours after start. Those settled quite differently within the first 30 minutes, where the borderline for Clay8_0%F_clay-H2O settled slower than for Clay8_0-1F_clay-H2O and Clay4Silt4_0-1F_claysilt-H2O.

Interestingly, borderlines for those three mixtures showed relatively similar settling rates to slow down after around 1 hour after which settling followed an gradual rate. However, Clay8_0%F_clay-H2O settled minimally faster for the rest of the 24 hours finally dropping 3ml below the value for Clay8_0-1F_clay-H2O.

At the of the experiment, layer thicknesses for the different mixtures were as presented in *Table 3*:

Table 3: Layer thicknesses for the different mixtures after 24 hours

Layer thickness:	Clay8_0%F	Clay8_0-1F	Silt8_0-1F	Clay4Silt4_0-1F
Fines [ml]	40	40	16	34
Sand [ml]	95	98	89	98

Comparison of layer thicknesses for sand show thicknesses of same magnitude for all mixtures, although the layer for Silt8_0-1F is a little smaller (89ml). There is more variation among mixtures for the fines particle layers, where Silt8_0-1F exhibit the smallest layer (16ml) and also Clay4Silt4_0-1F is 6ml smaller than the 8% clay mixtures (both 40 ml).

5 Debris flow fan experiment

Another main part of this study was the conduct of debris flow fan experiments, which should help to investigate the influence of composition and content of fine particle sizes of debris flows on flow dynamics, fan building processes and deposition characteristics of alluvial fans.

5.1 Introduction of ongoing project

Debris flow fan experiments were carried out within the framework of an ongoing project as described by Chen et.al (2022). In their study they investigated how clay content may be related to differences in avulsion controls. For doing so, they, among other methods, performed down-scaled laboratory experiments, where alluvial fans were built by long-term and incremental debris flows. Their research found:

- (1) Decreasing fine particle content increases the variability of fan slopes and associated channelization dynamics.
- (2) For all mixtures long-term continuous alluvial fan experiments form more complex surface channelization than repeated flows for the same total time, indicating the importance of both particle sizes and timescales on alluvial fan surface morphology.

In their summary, they mention potential scaling effects of the small particles in the overall size distribution as silt and clay particles are different (settling velocities, relative interparticle interactions) and therefore would affect larger-scale flows. Moreover, they predict that investigations of physical processes (micro-scale, interparticle dynamics) of silt and clay can help to evaluate how fine and larger-particle interactions influence macro-scale fan morphologies. However, their results motivate consequential research to be followed in the future as they provide insights to design experiments more in-line with particular field-scale fan development.

5.2 Debris flow fan experiments

5.2.1 Methodology

Based on findings summarized in chapter 1 and motivated by the ongoing research project (Chen et. al 2022), it was of interest to further investigate alluvial fan development related to variations of debris flow mixtures. Therefore, new debris flow fan experiments were carried out, which were performed using the laboratory experimental set-up from Chen et. al (2022). This means, an already existing experimental set-up served for the experiments, and thus, general information about experimental set-up and procedure, which were true for this study as well, can be found in that paper.

However, the new experiments also included some modifications. On the one hand, there were made improvements of the set-up and procedure and on the other hand, new ideas and questions lead to more complex analyses techniques. Those adaptations and this study specific methodology will be described and introduced below.

For the mixtures of the debris flow fan experiments the same materials (sand, silt, clay and PDADMAC) were used as for the Slump Slurry experiments, as described in chapter xx. Four experiments (mixtures A, B1, B2, C) were performed using three different mixtures which varied regarding fines particle size (clay, silt), presence of flocculant (0%, 0.1%) and the experiment duration (5min, 15min). In general, the ratio (by mass) for all mixture compositions was sand/(water + fines) = 50/(46 + 4) i.e. solid/(fluid) = 50/50; the fines content for each mixture was 8%/fluid by mass (=4% of the total mass). Those ratios are similar but (slightly) different to those of the Slump Slurry mixtures, where mixtures containing 8%fines/fluid ($\approx 4.1\%$ of the total mass) show a ratio solid/fluid = 48.7/51.3).

In general, the experimental runs were carried out as continuous flows for 15 minutes (mixtures B1, B2,C), whereas one experiment (mixture A) ran 5 minutes. Following an overview of the experiments and mixtures is presented:

Table 3: Overview of debris flow fan experiments and their mixture compositions

experiment	Date	Sand	Water	Clay	Silt	Flocculant	Flow duration
t	[mm/dd]	[%]	[%]	[%]	[%]	[%]	[min]
A	04/11	50	46	4	-	-	5
B1	06/09	50	45.996	4	-	0.1	15
B2	06/23	50	45.996	4	-	0.1	15
C	07/19	50	45.996	-	4	0.1	15

Improvements of the set-up basically included the installation of a new permeable layer and the change from a U-shape to a V-shape of the chute. The new permeable layer was made of #200 mesh filter screen sheet, which was fixed on lattice tiles covering an area of approximately 2x2m.

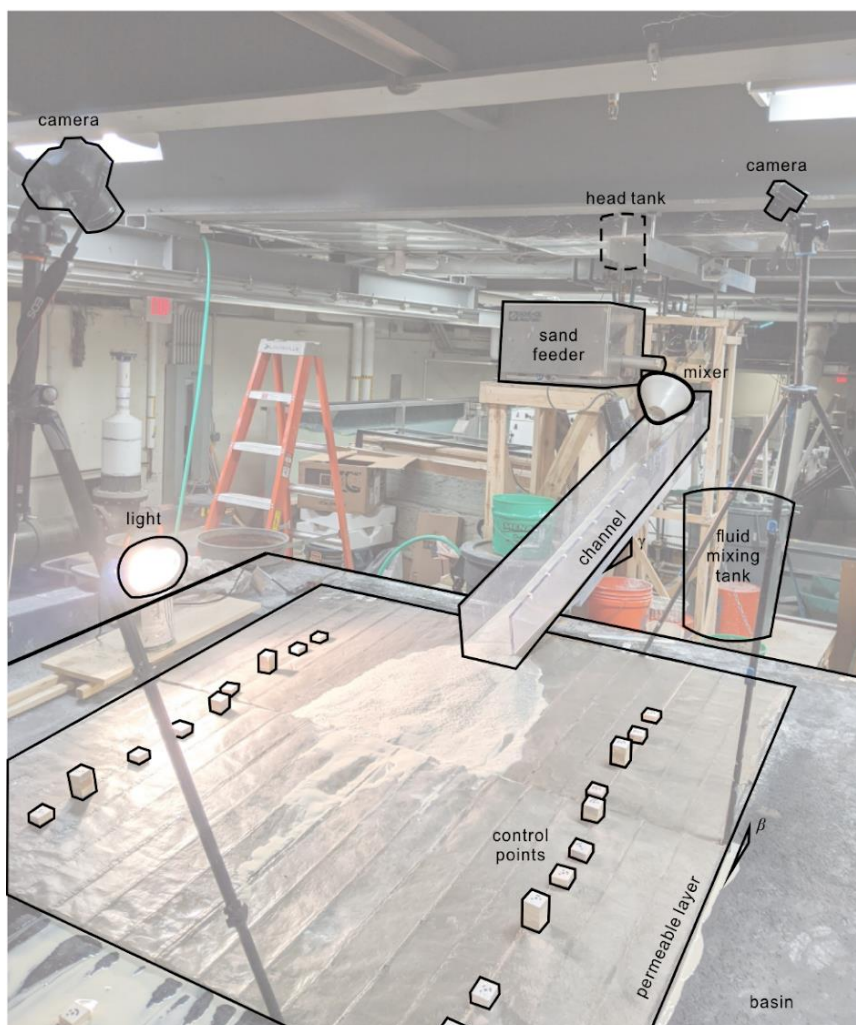


Figure 7: Existing experimental set-up (Chen et al. 2022) presenting instruments and tools to produce debris flow fans. Figure from Chen et al. (2022).

For data collection, a photogrammetric approach was used to obtain high resolution topographic maps of the surface of the experimental fans. This is often called a “Digital Elevation Model” (DEM) in the literature. To obtain high resolution DEM’s, Chen et al. (2022) took over 100 photographs with a high resolution camera of the debris fan surface and topographic markers.

Software was used to convert the images into a DEM whose resolution was 2mm by 2mm in plan view and 1.5 mm resolution normal to the bed. With the set-up used in the 2022 paper, Chen, et al. (2022) were able to obtain DEM's and orthonormal pictures of the fan surface at the end of the run, though it could not provide data throughout the experiments.

Prior to the beginning of this project a new approach was developed to build DEM fans at high frequency throughout the run, as the fan was developed (Hung et al., 2022). While the apparatus for this real-time photogrammetric data acquisition was developed, it still needed assembly and trouble shooting in February, 2022. Hence, the first part of the work performed for this visit was assisting in these tasks. More detail will be included in the Master's Thesis (Scheiber, 2023) and the Experiments in Fluids paper under development.

This new approach should be able to not just build one DEM of the resulted fans in the end of each experiment, but rather to generate DEMs for certain time steps of interest, to also investigate fan building processes. This could be accomplished by a complex photogrammetry set-up which then made it possible to dynamically build DEMs for any desired time step throughout the duration of the experiment.

The assembly and trouble shooting was threefold. It involved assembly of a reliable arrangement of cameras and lighting unique to the needs of data acquisition up to one hour long. It also included use of coloring techniques for improved imaging as well as markers necessary for DEM building.

Moreover, a laser cart installed on the ceiling of the laboratory hall at SAFL enabled necessary topographical scans of the deposition area, which was used in order to scan the calibration markers and calibrate the cameras before starting the experiment.

The procedure to carry out the debris flow fan experiments basically included two parts, (1) debris flow fan set-up and (2) photogrammetry set-up, whereas both parts overlap in their experimental order. Some information to part (1), regarding experimental works such as preparation and circulation of the fluid, is already described in the paper from Chen et. al (2022). Following, the experimental procedure will be introduced:

For experimental preparation, two key mixture components are considered. The first is angular sand of approximately 1mm in diameter. The second is a fluid comprised of water, clay, and flocculant. The last component is a flocculant that helps the clay settle in the experiments over a more comparable timescale that takes place in the larger field debris flows. For long-term flows of reliable mixture content, the clay, water and flocculant are mixed well and continuously prior to the experimental set-up. The outlet of the mixing system is calibrated and tested throughout the experiments to assure a uniform mixture throughout. Also, before the experiments are initiated, the output of the sand feeder is measured and tested to assure a uniform mixture.

When the experiments are initiated, both the sand and the clay/flocculant/water mixture are input separately and simultaneously into a mixing funnel. During the first few seconds of the experiment and at intervals of 5 minutes, the output of the funnel mixer is sampled to assure that the ratio does not change throughout the experiment. Then the timing is begun and flow into the channel proceeds.

After the experiment was finished, cameras were turned off and some qualitative observations were made of the fan so it could be compared with other experimental results. Then, cleaning could be commenced.

In total, the time spent on one experimental run (15min), including preparation and cleaning up the basin was about 6 hours at least.

Data processing and analysis of experimental fans

The aim of data processing basically was to convert the raw videos into DEM's. For doing so, some calculations needed to be done in MATLAB and then the full array of pictures were inputted into a commercial software (Agisoft Metashpe). In a final step, MATLAB was used to convert the DEM's into visualized topographic contour maps.

Data analysis focused on obtaining debris flow dynamics (avulsion) and fan building processes. For that, contour maps at different time steps and videos were interpreted qualitatively to investigate physical processes and to compare the morphology of alluvial fans among the experiments.

5.2.2 Results: Qualitative comparison of debris flow fans

For the following comparison, contour plots of experiment B1 were chosen for analysis. Since control samples for B2 show slight changes in ratios in the end of the experiment, B1 might be more reliable to represent 4% clay_0.1%Flocc.

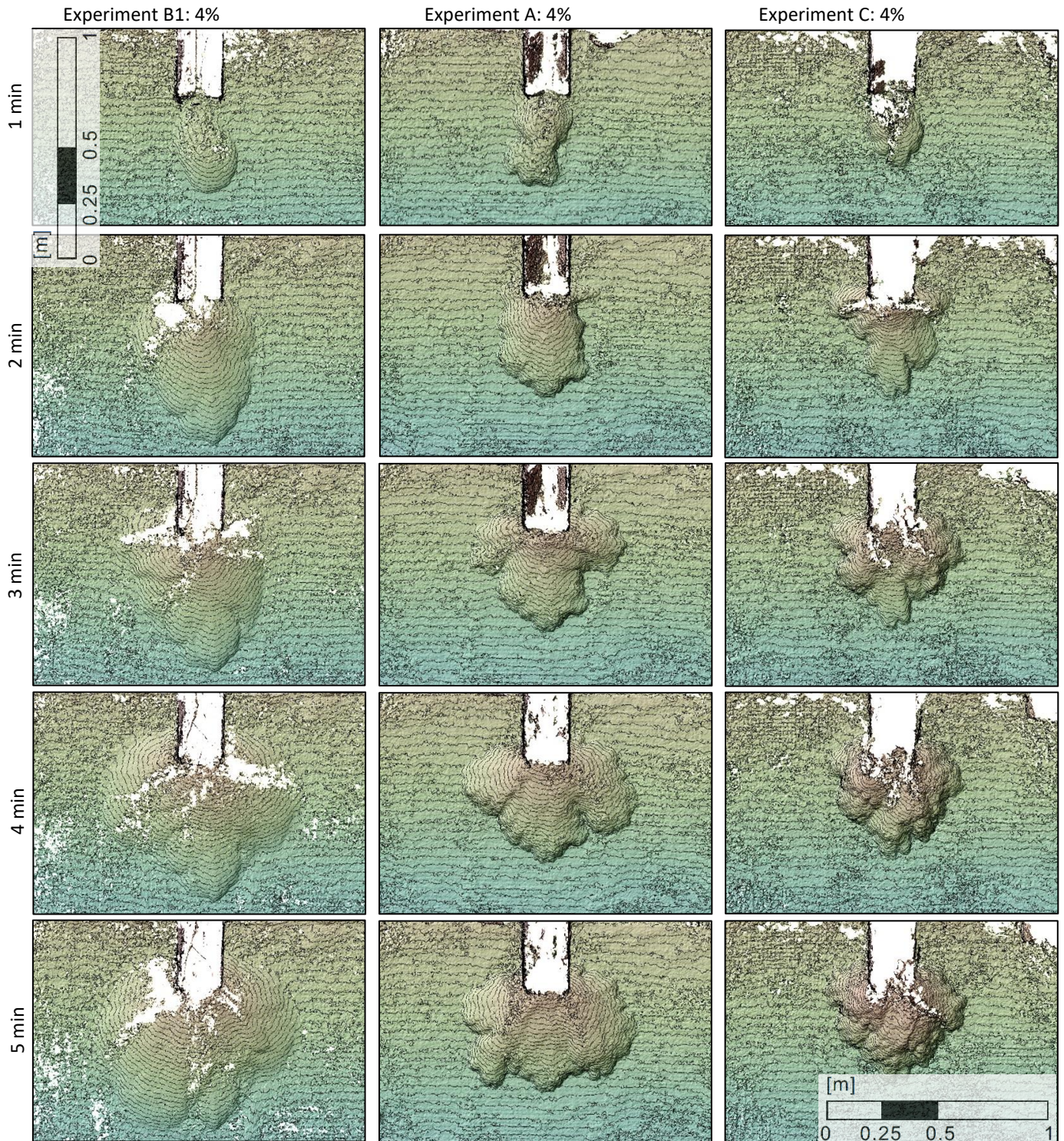


Figure 8: Comparison of contour plots (contour = 5mm) of debris flow fan experiments A (4% clay_0.1%Flocc), B (4% clay_0%Flocc) and C (4% silt_0.1%Flocc) for 5 and 15 minutes respectively

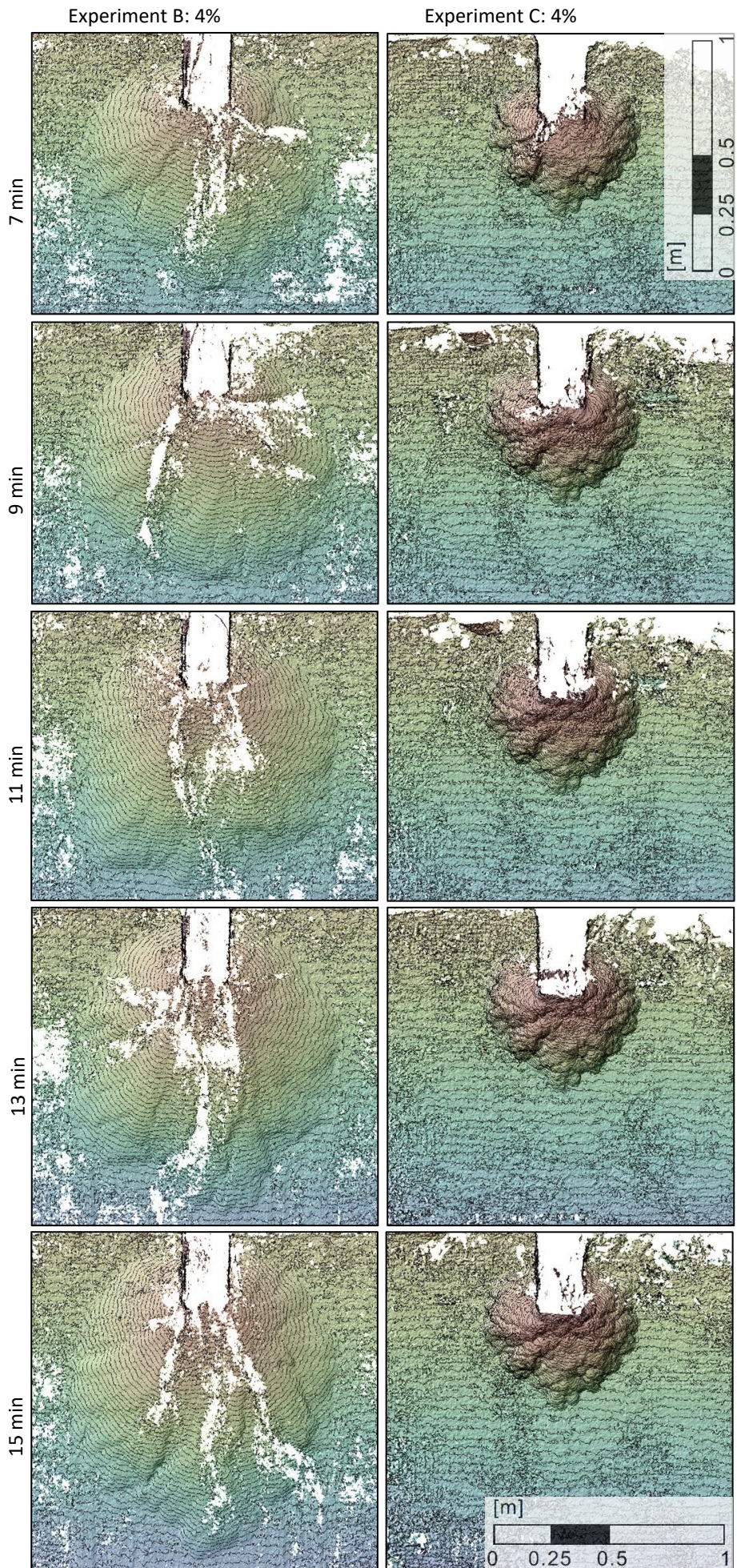


Figure 9: Continuation of comparison of contour plots (contour = 5mm) of debris flow fan experiments B (4% clay_0%Floc) and C (4% silt_0.1%Floc) for minutes 7, 9, 11, 13 and 15.

White area in contour plots in *Figure 8* and *Figure 9* is area without any data, through insufficient texture on the fan surface such as homogeneous surface without any food color or moving material in flow channels.

Analyzed videos for the 5 minutes of experiment A (4% clay_0%Floc) basically showed relatively short (apex near) debris flow runout caused by immediate aggradation and deposition leading to channel in-filling, up-fan aggradation, channel plugs and finally to channel diversion. This is displayed in contour maps (minutes 1-5) *Figure 8*, where after 2 minutes the flow avulsed, split up into 2 flows so that the fan grew to the left and the right (flow direction) forming typical lobes.

Videos for experiment C (4% silt_0.1%Floc) exhibited similar flow and deposition behavior as experiment A. However, debris flow runout and deposition of material and drainage of fluid seemed to occur even faster as in A. Backstepping, channel blockage and avulsion built the base of the fan within the first 3-4 minutes. From minute 5-9, flows developed additional lobes and snouts, letting the fan grow mainly in vertical direction while the area of the fan surface only slightly expanded. During that process (1-9 minutes), mostly two flows, split by a channel plug at the fan apex, shifted from the fan sides (right and left) toward the center of the fan, merging to one big flow for only a short time to split up and again shift sideways in the same manner. From minutes 9-10, flows were not flowing beyond the apex so that from then on deposition only occurred from the apex upwards into the chute. Therefore, contour plots from minutes 9-15 did not change anymore *Figure 9*.

As for experiment B (4% clay_0.1%Floc), videos showed quite homogeneous fan development in the beginning of the experiment. Compared to A and C, backstepping and channel aggradation begun later at around 2 minutes, splitting the main flow in two flows going left and right (3 minutes). In the following minutes 4-15, the mostly two flows avulsed and channels shifted from the fan sides (right and left) toward the center of the fan, merging to one big flow until splitting up and shifting sideways again. That process repeated a few times resulting a quite symmetric fan.

Contour plots for minute 5 (*Figure 8*) in general displayed a smooth surface for B, showing some shallow lobes and channels, whereas fan surface of experiment A is more irregular and very irregular and bumpy for experiment C. Total fan area 15 minutes (*Figure 9*) followed the trend of fan surface bumpiness, as the area for B is by far greater than for C. The same goes for fan slopes as contour lines indicate the slightest fan slopes for B and the steepest for C.

6 Discussion

6.1 General interpretation of data from material tests

There is an impact on settling behavior among the mixtures as settling for silt particles of the mixture Silt8_0-1F occurred faster whereas fines particles of mixtures containing clay were suspended (still settling) throughout the experiment. Hereby, fines particles of Clay4Silt4_0-1F settled faster than the clay particles of Clay8_0-1F and of Clay8_0%F, which were the latest to settle (probably due to flocculant effect). This observation is not expected as silt settles faster than clay particles due to their diameter and the mineral characteristics of clay. Those differences in settling behavior caused by fines particle **composition** might affect physical processes and flow dynamics forming alluvial fans (**morphology**).

Material tested in the course of Slump Slurry tests also showed effects of fines content variation on area, perimeter and complexity index. Results from Slump Slurry tests revealed trends for area and perimeter to increase with the proportion of silt/fluid and decrease with the amount of clay/fluid respectively. Similarly, clayey mixtures ($\geq 50\%$ clay/fines) created less irregular and smoother perimeter than silty mixtures, since values of N_b increase with the proportion of silt and decrease with the amount of clay respectively. Those findings indicate viscous effects of increased clay content on the slurry, whereas silt seems to cause the opposite, as the complexity sharply increased as soon as the mixtures became more silty ($>50\%$ silt/fines). Those trends indicate consequences for flow dynamics depending on fines **composition** (silt and clay) of the debris flow material.

Furthermore, Slump Slurry results also pointed out, that N_b values for 16% fines/fluid mixtures were smaller than for 8% fines/fluid mixtures, independently from their flocculant content. Possible explanations for that might be the difference between the water and fines content, as mixtures consisting of less fines but more water (watery mixtures) have a more irregular perimeter than mixtures containing more fines but less water (thicker mixtures). This idea goes along with results of area and perimeter exhibiting higher values for mixtures of 8% fines/fluid than for 16% fines/fluid mixtures, supporting the theory that an increase in **fines content** affect the consistence of mixtures to be thicker and more viscous.

For interpretation of the results, it is important to consider the role of **flocculant** in some material mixtures, which was used with regard to scaling of the debris flow fan experiment (Chen et. al 2022). In this context, the influence of flocculant on the material mixtures were visible in the following: Flocculant appeared to have a viscous impact on the mixture with clay as it would keep the particles together, forming slurries with less irregular perimeters and smaller areas. In contrast, when mixtures were silty, a rather opposite effect could be observed since N_b values were the greatest for silty mixtures containing 1%. For example, there were higher values for silty mixtures of 8% fines/fluid (i.e., 4.44 and 6.27) for 1% flocculant compared to mixtures of 0.1% flocculant. Furthermore, an expected impact of flocculant is demonstrated by the finding, that the borderline for Clay8_0%F_clay-H2O (without flocculant) settled slower than for Clay8_0-1F_clay-H2O and Clay4Silt4_0-1F_claysilt-H2O (with flocculant).

6.2 Discussion on data of debris flow fan experiments

In this study material characterization tests and debris flow fan experiments helped to answer the research questions of (1) how changing fines **particle content** and **composition** (complementing silt) in debris flows influence flow dynamics (in particular **avulsion**) of debris flows, and (2) how these differences in debris flow behavior affect **deposition characteristics** and the **morphology** of alluvial fans?

In general, results for all experiments showed a coherent **avulsion** pattern of channel blockage, backstepping or up-fan aggradation and channel in-filling, avulsion and establishment of a new active channel (channel diversion) as reported by De Haas et al. (2018) and Whipple and Dunne (1992). This means that mainly avulsion mechanism (2) (gradual shifting) of channel and locus of deposition, was responsible for fan building processes. This observation, that there occurred no avulsion mechanism (1) (abrupt shift), might be reasonable because the experimental set-up was with continuous and constant fluid discharge and no surges. This is consistent with Hubert and Filipov (1989) and De Haas et al. (2018) who explained that abrupt shifts would be expected in scenarios of debris flow surges.

Observations showed debris flow runout to be the shortest for experiment C (4% silt_0.1%Flocc) followed by A (4% clay_0%Flocc), which is in contrast to B (4% clay_0.1%Flocc), where flow runout was longer resulting in bigger depositional fan formation. Results show that gradual shifting produced channel plugs at the apex especially for experiment C, so that material flows could not go beyond the plug (from minute 9) and material deposited in the chute. Similar plug was formed at the apex for A (5min duration only), whereas in contrast, no such plug at the apex built up for experiment B and thus, flows shifted on the fan surface throughout the experimental duration (15 min). These plugs influenced the fan surface as debris flows were able (experiment B) or not (experiment A) to reach the fan which inhibited **avulsion**.

These findings of differences in runout and plug formation among the mixtures might go along with the study from Whipple and Dunne (1992), who indicated, that the **fine particle fraction** (silt-clay) is critical to retention of water within the slurry and, hence, is the most important textural control on flow mobility. Also, Kaitna et al. (2016) found that debris flow mixtures containing a GSD of coarse fraction including fine particles in the fluid strongly influence the presence of sustained excess fluid pressure, which in turn affects bulk flow resistance of debris flows. In the same context, De Haas et al. (2015) revealed that runout enhanced with an increase in clay fraction, probably because of better retained excess pore pressures.

Here, this could mean that this critical retention of water within the slurry and linked pore pressures were governing debris flow fan experiments. In this regard, similar characteristics (retention of water within the slurry) were seen in material tests which revealed viscous effects when increasing clay and flocculant content in the mixture. For example, viscous effects of increased clay content ($\geq 50\%$ clay/fines) on the slurry were observed, whereas silt seemed to cause the opposite, as the complexity sharply increased as soon as the mixtures became more silty ($>50\%$ silt/fines). Also, results from Slump slurry tests showed a viscous effect of flocculant on clayey mixtures as it would keep the particles together, forming slurries with less irregular perimeters and smaller areas.

Therefore, the presence of clay and flocculant causing viscous effects might have been responsible for differences in debris flow fans between experiments B (4% clay_0.1%Flocc) and A (4% clay_0%Flocc) as well as for experiments C (4% silt_0.1%Flocc) and B (4% clay_0.1%Flocc). However, these viscosity effects must be interpreted carefully, as they showed different impacts on area in slurry results and area of fan experiments. While area of the slurries decreased (thicker

slurry) with increased clay content, fan area was the largest for experiment B (clay mixture), where fan deposited in thin layers. In contrast, mixtures containing little clay content (more silt) produced thicker deposits on a small area in the fan experiment (as for experiment C), whereas the same mixture resulted in a large area in the slump slurry investigations. This difference might be caused by the boundary condition of the deposition layer, which was a permeable layer/permeable fan surface for fan experiments and a non-permeable metal board for the Slump Slurry tests, on which the silt-water fluid could not drain as it would in the debris flow fan experiment and spread all over the board. Therefore, those Slump Slurry results, in particular for silty mixtures, can not directly be connected to a debris flow experimental or natural setting.

That experiment C (4% silt_0.1%Floc) exhibited the shortest runout and fan area agrees with a work from Chau et. al (2000) who found, that mixtures containing gravel, sand but also silt, were showing the shortest runout and the least spreading of deposition compared to the mixtures with coarser particle content (sand and gravel) so that shape and area of fan altered correspondingly in their experimental debris flows. Contributing to this, Iverson (2003) mentioned debris flows with little fine sediment to produce thicker deposits. In this context, results from settling tests demonstrated that silt settled faster than clay particles considering the different particles sizes as well as mineral characteristics of clay. This could indicate that silt does not interfere as part of the fluid with sand particles because of its fast settling behavior, whereas clay, according to settling results, is suspended and part of the fluid, which strongly influences the presence of sustained excess fluid pressure and therefore affects bulk flow resistance of debris flows as mentioned by Kaitna et al. (2016).

All together, this affects **deposition characteristic** and fan **morphology** as comparison of fan geometries (features, shape and area after 15 minutes) among the mixtures show, that the mixture (4% silt_0.1%Floc) of experiment C (bumpiest fan surface, smallest deposition area and steepest slopes) is very different to the mixture (4% clay_0.1%Floc) of experiment B (smooth fan surface, large deposition area and moderate slopes).

These findings are in agreement with Chen et al. (2022) who demonstrated the importance of fine particle content as the increase of clay content decreases diversity of fan slopes and associated channelization dynamics and therefore leads to smoother fan surface. However, examinations from De Haas et al. (2015) also showed that too large proportions of clay (>0.22) make debris flows highly viscous so that runout is reduced. This is reasonable as Slump Slurry results showed this viscous trend for mixtures containing high fines content of clay as well as results of area and perimeter exhibiting higher values for mixtures of 8% fines/fluid than for 16% fines/fluid mixtures, indicating that an increase in clay content affect the consistence of mixtures to be thicker and more viscous.

In any case, scaling effects of conducted debris flow fan experiments need to be considered when interpreting the relevance of investigations, as the scale and experimental conditions play a crucial role at understanding the behavior of debris flows (Iverson, 2015). For instance, this experimental set-up mimicked continuous debris flows rather than a more natural behavior as are flows in surges. Also, mixture compositions did include only one fine particle size (clay or silt), whereas it is likely that there is mostly a combination of silt and clay in a natural setting.

Moreover, all comparisons of silt and clay particles should always consider not only the physical differences in particle sizes, but also the chemical properties of clay, which silt do not have.

7 Conclusion

In this study laboratory experiments on alluvial fan development and desk-top experiments on material characterization of the sediment-water mixtures have been carried out. The results suggest that retention of water (Whipple & Dunne, 1992) and retained excess of pore pressures within the slurry (Kaitna et al., 2016; De Haas et al., 2015) have strong effects on the deposition pattern of the mixtures. According to the presented Slump Slurry experiments, these **viscous effects** are caused by the presence of **clay** and flocculant, but not the **silt**. However, explained in the discussion section, viscosity effects must be interpreted carefully as Slump Slurry results, in particular for silty mixtures, can not directly be connected to a debris-flow experimental or natural setting.

Settling tests indicate that **silt** might not interfere as part of the fluid with sand particles because of its fast settling behavior and therefore could be responsible for higher bulk flow resistance of debris flows, as seen in experiment A (4% silt_0.1%Flocc).

Comparison of debris flow fan experiments highlighted the influence of mixture composition (**silt vs. clay**) on **debris-flow behavior**. **Runout** distances for experiment A (4% silt_0.1%Flocc) were shorter than for B (4% clay_0.1%Flocc), where flow runout was longer resulting in larger depositional fan formation. Another influence of fines composition was **plug formation** at the apex, which was created by gradual shifting especially for experiment C (4% silt_0.1%Flocc). In that case, this plug influenced the fan surface as flows could not reach the fan surface anymore so that **avulsion** was not possible (after 9 minutes).

Debris flow fan experiments mainly produced **avulsion** mechanism (2) (gradual shifting) of channel and locus of deposition, which most likely is caused by the experimental set-up of continuous and constant fluid discharge without surges. Data from debris flow experiments also revealed different effects of **mixture compositions (silt vs. clay)** on **deposition characteristic** and fan **morphology**. Experiment A (4% silt_0.1%Flocc) showed the bumpiest fan surface, smallest deposition area and steepest slopes compared to Experiment B (4% clay_0.1%Flocc), which exhibited smooth fan surface, large deposition area and moderate slopes.

Future works could consider using a permeable layer for Slump Slurry tests to better mimic experimental or natural conditions. Along with this, it might be interesting to perform experiments with different flow conditions, where debris flows would proceed in form of surges instead of continuous flows. Furthermore, additional research could consider to test mixtures containing silt and clay in debris flow fan experiments.

Acknowledgements

I would like to express my thanks to the Austrian Marshall Plan Foundation for awarding me this scholarship, which made this research possible but also strengthened collaboration between my home university and the host institution.

I am very grateful to my supervisor Prof. Roland Kaitna who made this research project possible. Thanks for the support in my wish to go abroad for doing research in the field of Mountain Risk Engineering. Only his collaboration allowed me to visit the U.S. Thanks for the mentoring and expertise throughout the period of my research.

I am very thankful to my co-supervisor Prof. Kimberly Hill for all her help and guidance in my research, which was connected to a National Science Foundation (NSF) funded research project (“MCA: Multi-scale considerations of climatic signatures in debris flows and alluvial fans”, August 1, 2021 thru July 31, 2024). Thanks for giving me the chance to do research at the renowned St. Anthony Falls Laboratory at the University of Minnesota and for allowing me to support field work in California. Along with this, I would like to thank all the staff at the lab who supported me and helped to develop a functional experimental set-up. Thanks to all my students friends at the lab for socializing and nice moments.

Hereby, special thanks to my generous research buddy, Tzu-Yin Chen, who provided several methodological tools for data processing and ideas which benefit my work, too. She influenced me as I learned so many things from her during our daily work in the lab – I wish her all the best for her career.

And finally, thanks to the most important people, especially to my parents, family and friends who have provided emotional, moral, material and financial support throughout the progress of my master’s research journey

References

- Austrian Standards (2019). *Testing fresh concrete: Part 5: Flow table test* (ÖNORM EN 12350-5:2019-06). Vienna. Austrian Standards International.
- Beaty, C. B. (1963). ORIGIN OF ALLUVIAL FANS, WHITE MOUNTAINS, CALIFORNIA AND NEVADA. *Annals of the Association of American Geographers*, 53(4), 516–535.
<https://doi.org/10.1111/j.1467-8306.1963.tb00464.x>
- Blair, T. C., & McPherson, J. G. (2009). Processes and Forms of Alluvial Fans. In A. J. Parsons & A. D. Abrahams (Eds.), *Geomorphology of Desert Environments* (pp. 413–467). Springer Netherlands. https://doi.org/10.1007/978-1-4020-5719-9_14
- Cavalli, M., & Marchi, L. (2008). Characterisation of the surface morphology of an alpine alluvial fan using airborne LiDAR. *Natural Hazards and Earth System Sciences*, 8(2), 323–333.
<https://doi.org/10.5194/nhess-8-323-2008>
- Chau, K. T., CHAN, L. C. P., LUK, S. T., & WAI, W. H. (2000). Shape of deposition fan and runout distance of debris flow: Effects of granular and water contents. In (pp. 387–395). A.A.Balkema, Brookfield.
- Chen, T.-Y., Hung, C.-Y., Mullenbach, J., & Hill, K. (2022). Influence of Fine Particle Content in Debris Flows on Alluvial Fan Morphology (under review).
- Costa, J. E. (1984). Physical Geomorphology of Debris Flows. In J. E. Costa & P. J. Fleisher (Eds.), *Developments and Applications of Geomorphology* (pp. 268–317). Springer Berlin Heidelberg. https://doi.org/10.1007/978-3-642-69759-3_9
- Costa, J. E. (1988). Rheologic, geomorphic, and sedimentologic differentiation of water floods, hyperconcentrated flows, and debris flows.
<https://eurekamag.com/research/019/925/019925764.php>
- De Haas, T., Braat, L., Leuven, J. R. F. W., Lokhorst, I. R., & Kleinhans, M. G. (2015). Effects of debris flow composition on runout, depositional mechanisms, and deposit morphology in laboratory experiments. *Journal of Geophysical Research: Earth Surface*, 120(9), 1949–1972.
<https://doi.org/10.1002/2015JF003525>
- De Haas, T., Densmore, A. L., Stoffel, M., Suwa, H., Imaizumi, F., Ballesteros-Cánovas, J. A., & Wasklewicz, T. (2018). Avulsions and the spatio-temporal evolution of debris-flow fans. *Earth-Science Reviews*, 177, 53–75. <https://doi.org/10.1016/j.earscirev.2017.11.007>
- De Haas, T., van den Berg, W., Braat, L., & Kleinhans, M. G. (2016). Autogenic avulsion, channelization and backfilling dynamics of debris-flow fans. *Sedimentology*, 63(6), 1596–1619. <https://doi.org/10.1111/sed.12275>
- Denny, C. S. (1967). Fans and pediments. *American Journal of Science*, 265(2), 81.
<https://doi.org/10.2475/ajs.265.2.81>
- Drew, F. (1873). Alluvial and Lacustrine Deposits and Glacial Records of the Upper-Indus Basin. *Quarterly Journal of the Geological Society*, 29(1-2), 441–471.
<https://doi.org/10.1144/GSL.JGS.1873.029.01-02.39>
- Dühnforth, M., Densmore, A. L., Ivy-Ochs, S., Allen, P. A., & Kubik, P. W. (2007). Timing and patterns of debris flow deposition on Shepherd and Symmes creek fans, Owens Valley, California, deduced from cosmogenic ¹⁰Be. *Journal of Geophysical Research*, 112(F3).
<https://doi.org/10.1029/2006JF000562>
- Hill, K. M., Gioia, G., & Amaravadi, D. (2004). Radial segregation patterns in rotating granular mixtures: Waviness selection. *Physical Review Letters*, 93(22), 224301.
<https://doi.org/10.1103/PhysRevLett.93.224301>
- Hill, K. M., Khakhar, D. V., Gilchrist, J. F., McCarthy, J. J., & Ottino, J. M. (1999). Segregation-driven organization in chaotic granular flows. *Proceedings of the National Academy of Sciences of*

- the United States of America*, 96(21), 11701–11706.
<https://doi.org/10.1073/pnas.96.21.11701>
- Hill, K. (2021). *MCA: Multi-scale considerations of climatic signatures in debris flows and alluvial fans (Project information about an ongoing project)*.
- Hooke, R. L. (1967). Processes on Arid-Region Alluvial Fans. *The Journal of Geology*, 75(4), 438–460.
<https://doi.org/10.1086/627271>
- Hubert, J. F., & Filipov, A. J. (1989). Debris-flow deposits in alluvial fans on the west flank of the White Mountains, Owens Valley, California, U.S.A. *Sedimentary Geology*, 61(3-4), 177–205.
[https://doi.org/10.1016/0037-0738\(89\)90057-2](https://doi.org/10.1016/0037-0738(89)90057-2)
- Hung, C.-Y., Chen, T.-Y., Scheiber, M., & Hill, K. (2022). Experiments in Fluids (in development).
- Hungr, O., Evans, S. G., Bovis, M. J., & Hutchinson, J. N. (2001). A review of the classification of landslides of the flow type. *Environmental & Engineering Geoscience*, 7(3), 221–238.
<https://doi.org/10.2113/gseegeosci.7.3.221>
- Iverson, R. M [R. M.]. (2003). *The debris-flow rheology myth*.
<http://pubs.er.usgs.gov/publication/70024614>
- Iverson, R. M [R. M.] (2015). Scaling and design of landslide and debris-flow experiments. *Geomorphology*, 244, 9–20. <https://doi.org/10.1016/j.geomorph.2015.02.033>
- Iverson, R. M [Richard M.], Reid, M. E., Logan, M., LaHusen, R. G., Godt, J. W., & Griswold, J. P. (2011). Positive feedback and momentum growth during debris-flow entrainment of wet bed sediment. *Nature Geoscience*, 4(2), 116–121. <https://doi.org/10.1038/ngeo1040>
- Jackson, L. E. J., Kostaschuk, R. A., & MacDonald, G. M. (1987). Identification of debris flow hazard on alluvial fans in the Canadian Rocky Mountains. In J. E. Costa & G. F. Wieczorek (Eds.), *Debris Flows/Avalanches* (Vol. 7, p. 0). Geological Society of America.
<https://doi.org/10.1130/REG7-p115>
- Kaitna, R., Palucis, M. C., Yohannes, B., Hill, K., & Dietrich, W. E. (2016). Effects of coarse grain size distribution and fine particle content on pore fluid pressure and shear behavior in experimental debris flows. *Journal of Geophysical Research: Earth Surface*, 121(2), 415–441.
<https://doi.org/10.1002/2015JF003725>
- Marchi, L., Pausto, A., & Tecca, P. R [Pia R.] (1993). Flow processes on alluvial fans in the Eastern Italian Alps. *Zeitschrift Für Geomorphologie*, 37(4), 447–458.
<https://doi.org/10.1127/zfg/37/1993/447>
- Marchi, L., & Tecca, P. R [P. R.] (1995). Alluvial fans of the Eastern Italian Alps: morphometry and depositional processes. *Geodinamica Acta*, 8(1), 20–27.
<https://doi.org/10.1080/09853111.1995.11105270>
- Melton, M. A. (1965). Debris-Covered Hillslopes of the Southern Arizona Desert: Consideration of Their Stability and Sediment Contribution. *The Journal of Geology*, 73(5), 715–729.
<https://doi.org/10.1086/627112>
- Pederson, C. A., Santi, P. M., & Pyles, D. R. (2015). Relating the compensational stacking of debris-flow fans to characteristics of their underlying stratigraphy: Implications for geologic hazard assessment and mitigation. *Geomorphology*, 248, 47–56.
<https://doi.org/10.1016/j.geomorph.2015.06.030>
- Scheiber, M. (2023). *Influence of debris-flow material composition on the morphology of depositional fans (in development)*.
- Tsunetaka, H., Hotta, N., Sakai, Y., & Wasklewicz, T. (2022). Effect of debris-flow sediment grain-size distribution on fan morphology. *Earth Surface Dynamics*, 10(4), 775–796.
<https://doi.org/10.5194/esurf-10-775-2022>

Whipple, K. X., & Dunne, T. (1992). The influence of debris-flow rheology on fan morphology, Owens Valley, California. *GSA Bulletin*, 104(7), 887–900. [https://doi.org/10.1130/0016-7606\(1992\)104<0887:TIODFR>2.3.CO;2](https://doi.org/10.1130/0016-7606(1992)104<0887:TIODFR>2.3.CO;2)